Generalization of Discrete-Time Wirtinger Inequalities and A Preliminary Study of Their Application to SNR Analysis of Sinusoids Buried in Noise

Kaveh Mollaiyan

A Thesis

in

The Department

of

Electrical and Computer Engineering

Presented in Partial Fulfillment of the Requirements for
the Degree of Master of Applied Science at
Concordia University
Montreal, Quebec, Canada

April 2008

Your file Votre référence
ISBN: 978-0-494-42494-0
Our file Notre référence
ISBN: 978-0-494-42494-0

ABSTRACT

Generalization of Discrete-Time Wirtinger Inequalities and A Preliminary Study of Their Application to SNR Analysis of Sinusoids Buried in Noise

Kaveh Mollaiyan

Sinusoidal signals have been always of interest because of their extensive applications in different areas of engineering and science. This research aims at generalizing the discrete Wirtinger inequalities and assessing their applicability in estimating the SNR of sinusoids of rational frequency $\frac{M}{N}\pi$ buried in additive noise.

The solution to the problem of estimating the SNR of a sinusoid of frequency $\frac{\pi}{N}$, corrupted with additive white noise, has been provided in the form of an inequality-based method. The limitations of using the existing inequalities in the proposed method have been discussed and modifications have been made to the existing Wirtinger inequalities accordingly. Generalizations of the modified inequalities have been achieved by changing the structure of the filter's impulse response. Performance curves with wider non-saturated regions have been obtained. By using reordering and modulation, an arbitrary sinusoid of frequency $\frac{M}{N}\pi$ has been converted to a sinusoid of frequency

$\frac{\pi}{N}$, allowing the proposed method to estimate the SNR of sinusoids of higher frequencies as well. The computational complexity of the proposed method has been evaluated and compared with a DFT-based approach.

Extensive simulation results showing the capability of the proposed method in estimating the SNR of an arbitrary sinusoid of rational frequency $\frac{M}{N}\pi$ have been provided. An advantage of the proposed method is that it can be adaptively adjusted to the length of the observed signal. In cases it is desired to evaluate the SNR of a sinusoid with a known frequency, the proposed method can be used as a computationally efficient option.

Acknowledgements

At First, I would like to thank my supervisor: Dr. Saed Samadi for his guidance and support. Your aptitude is appreciated.

Thanks to my wife for her love and patience. Invaluable and always remembered.

Many thanks to my father for inspiring and supporting me, and my mother for encouraging me.

Special thanks to everyone that helped me in preparing this thesis: Amir for his review and feedback.

Contents

List of Figures vi

List of Abbreviationss xii

1 Introduction 1

1.1 A Review of Methods of Estimation of Sinusoids 3

1.2 The History of Development of Theory of Wirtinger-Type Inequalities 7

1.3 Existing Wirtinger-Type Inequalities 8

1.4 Goals and Contributions of The Thesis 10

1.5 Organization of the Thesis 12

2 Derivation of Existing Discrete-Time Wirtinger Inequalities Using a DFT-Based Approach 14

2.1 Preliminary 15

2.1.1 DFT and Circular Convolution 15

2.1.2 Forward Difference Systems 16

2.2 Propositions of Wirtinger-Type Inequalities and Their Proofs 18

2.3 Derivation of Existing Discrete-Time Wirtinger Inequalities 22

3 Modification of Inequalities and Their Application to Estimation of SNR of Sinusoids **32**

3.1 Method of SNR Estimation of Sinusoidal Signals 33

3.2 Modification of Existing Inequalities 35

4 Generalizations of Discrete Wirtinger-Type Inequalities **46**

4.1 Generalization to Weighted Inequalities with Two Parameters 47

4.2 Other New Two-Parameter Inequalities 53

4.2.1 Two Weights with a Gap of One 53

4.2.2 Gap of Two 66

4.3 Inequalities with Three Non-Zero Weights 74

4.4 Summary 80

5 A Method for Estimating SNR of Sinusoids of Frequency $\frac{M}{N}\pi$ and Its Analysis **83**

5.1 Signal Reordering and Modulation for Frequency Downconversion . . 85

5.2 Optimum Impulse Response Coefficients of The Weighted Forward Difference System 87

5.3 Comparison with A Classical DFT-Based Approach 91

5.4 Computational Complexity 92

5.5 Analysis of the Error Due to Finite Duration of Observed Signal . . . 94

6 Conclusion and Future Work **98**

6.1 Conclusion 98

6.2 Future Work 100

List of Figures

2.1 $2 - 2\cos(2\pi k/N)$ for $N = 10$. 21

3.1 Block diagram of the proposed method for estimation of the SNR of a sinusoidal signal with known frequency. 34

3.2 Average performance curve for inequality 3.2.1 with $N = 32$. 37

3.3 Average performance curve for inequality 3.2.2 with $N = 32$. 40

3.4 Average performance curve for inequality 3.2.3 with $N = 32$. 42

3.5 Average performance curve for inequality 3.2.4 with $N = 32$. 44

4.1 $h_{wf}[n]$ - impulse response of the weighted forward difference system. . 47

4.2 Average performance curves for inequality 4.1.1 with (1) $a = b = 1$, (2) $a = 1$ and $b = 2$, (3) $a = 3$, $b = 1$, and $N = 32$. 49

4.3 Average performance curves for inequality 4.1.2 with (1) $a = b = 1$, (2) $a = 1$ and $b = 2$, (3) $a = 3$, $b = 1$, and $N = 32$, $\gamma = -\pi/2$. 50

4.4 Average performance curves for inequality 4.1.3 with ((1) $a = b = 1$, (2) $a = 1$ and $b = 2$, (3) $a = 3$, $b = 1$, and $N = 32$. 51

4.5 Average performance curves for inequality 4.1.4 with (1) $a = b = 1$, (2) $a = 1$ and $b = 2$, (3) $a = 3$, $b = 1$, and $N = 32$, $\gamma = -\pi/2$. 52

4.6 $h_{g1}[n]$ - impulse response of the system with a circular gap of one between the two non-zero weights. 54

4.7 $a^2 + b^2 - 2ab\cos(4\pi k/N)$ for $a = b = 1$, and $N = 16$. 55

4.8 Average performance curves for inequality 4.2.1 with (1) $a = b = 1$, (2) $a = 1$ and $b = 2$, (3) $a = 3$, $b = 1$, and $N = 32$. 57

4.9 $a^2 + b^2 - 2ab\cos(4\pi k/N)$ for $a = b = 1$, and $N = 17$. 58

4.10 Average performance curves for inequality 4.2.2 with (1) $a = b = 1$, (2) $a = 1$ and $b = 2$, (3) $a = 3$, $b = 1$, and $N = 33$. 59

4.11 $a^2 + b^2 - 2ab\cos(4\pi k/N)$ for $a = b = 1$, and $N = 18$. 61

4.12 Average performance curves for inequality 4.2.3 with (1) $a = b = 1$, (2) $a = 1$ and $b = 2$, (3) $a = 3$, $b = 1$, and $N = 34$. 63

4.13 $a^2 + b^2 - 2ab\cos(4\pi k/N)$ for $a = b = 1$, and $N = 19$. 64

4.14 Average performance curves for inequality 4.2.4 with (1) $a = b = 1$, (2) $a = 1$ and $b = 2$, (3) $a = 3$, $b = 1$, and $N = 35$. 65

4.15 $h_{g2}[n]$ - impulse response of the system with two zeros between the two weights. 66

4.16 $a^2 + b^2 - 2ab\cos(6\pi k/N)$ for $a = b = 1$, and $N = 18$. 67

4.17 Average performance curves for inequality 4.2.5 with (1) $a = b = 1$, (2) $a = 1$ and $b = 2$, (3) $a = 3$, $b = 1$, and $N = 30$. 68

4.18 $a^2 + b^2 - 2ab\cos(6\pi k/N)$ for $a = b = 1$, and $N = 19$ 69

4.19 Average performance curves for inequality 4.2.6 with (1) $a = b = 1$, (2) $a = 1$ and $b = 2$, (3) $a = 3$, $b = 1$, and $N = 31$. 70

4.20 (a) $a^2 + b^2 - 2ab\cos(6\pi k/N)$ for $a = b = 1$, $N = 20$, (b) $a^2 + b^2 - 2ab\cos(6\pi k/N)$ for $a = b = 1$, $N = 21$, (c) $a^2 + b^2 - 2ab\cos(6\pi k/N)$ for $a = b = 1$, $N = 22$ and (d) $a^2 + b^2 - 2ab\cos(6\pi k/N)$ for $a = b = 1$, and $N = 23$. 71

4.21 Average performance curves for inequality 4.2.7 with (1) $a = b = 1$, (2) $a = 1$ and $b = 2$, (3) $a = 3$, $b = 1$, and $N = 32$. 72

4.22 Average performance curves for inequality 4.2.8 with (1) $a = b = 1$, (2) $a = 1$ and $b = 2$, (3) $a = 3$, $b = 1$, and $N = 33$. 73

4.23 Average performance curves for inequality 4.2.9 with (1) $a = b = 1$, (2) $a = 1$ and $b = 2$, (3) $a = 3$, $b = 1$, and $N = 35$. 74

4.24 Impulse response of the system with input-output relation $y[n] = ax[n+2] + bx[n+1] + cx[n]$. 75

4.25 $\|H_{3t}[k]\|^2$ with $a = 2$, $b = 4$, $c = 1$, $N = 20$. 76

4.26 Average performance curves for inequality 4.3.1 with (1) $a = 2$, $b = 4$, $c = 1$, (2) $a = 1$, $b = 5$, $c = 3$, (3) $a = 3$, $b = 7$, $c = 2$, with $N = 32$. . 78

4.27 Average performance curves for inequality 4.3.2 with (1) $a = 2$, $b = 4$, $c = 1$, (2) $a = 1$, $b = 5$, $c = 3$, (3) $a = 3$, $b = 7$, $c = 2$, with $N = 32$. . 80

4.28 Average performance curves for inequality 4.3.2 with $N = 32$, $a = 3$, $c = 2$, and $b = 4, 5, \cdots, 8$. 81

5.1 Block diagram of the proposed method for estimation of the SNR of a sinusoidal signal with known rational frequency $\frac{M}{N}\pi$. 87

5.2 Average performance curve for inequality 4.1.1 with (1) $a = b = 1$ (2) $a = 1$ and $b = 2$ (3) $a = 3$ and $b = 1$, with $N = 32$, $M = 5$. 88

5.3 $|H_{wf}[k]|^2 = a^2 + b^2 - 2ab\cos(2\pi k/N)$, for $N = 20$ at different values of weights a and b. The dotted curves show the graphs in which $a \neq b$. . 89

5.4 Ratio of the two sides of inequality 4.1.1 vs. $\frac{b}{a}$ at different SNR values. 90

5.5 Average performance curve for inequality 4.1.1 using a classical DFT-based method for $N = 16$, with $a = b = 1$. 92

5.6 Average performance curves for inequality 4.1.1 using different lengths of the observed signal in table 5.1, with $a = b = 1$. 95

5.7 Average performance curves for inequality 4.1.3 using different lengths of the observed signal in table 5.1, with $a = b = 1$. 96

List of Abbreviations

ARMA ..... Autoregressive Moving Average

DFT ..... Discrete Fourier Transform

LMS ..... Least Mean Squares

LS ..... Least Squares

MA ..... Moving Average

MAFI ..... Matched-Filterbank

ME ..... Maximum Entropy

ML ..... Maximum Likelihood

QDE ..... Quadrature Delay Estimator

SNR ..... Signal-to-Noise Ratio

WLS ..... Weighted Least Squares

Chapter 1

Introduction

Estimating the signal-to-noise ratio (SNR) of an observed signal is required in many applications of signal processing and telecommunications. It can be used to provide the channel quality information required by power control, mobile assisted handoff, and adaptive modulation algorithms [1, 2]. SNR estimation methods are used in speech processing applications as well. The speech enhancement algorithms based on spectral decomposition methods, such as the maximum likelihood (ML) method, rely on the estimation of the background noise energy and the SNR in the various frequency bands [3].

Sinusoidal signals have been always of interest because of their extensive applications in different areas of engineering and science. For example, they are used in system identification as probing signals [4], where the amplitude of the sinusoids is estimated to find the coefficients of the transfer function of a system. Different estimators can be used for amplitude estimation, such as those based on the least squares (LS) method, weighted least squares (WLS) method, and matched-filterbank (MAFI)

approach [5–7]. Another application of sinusoid estimation is in evaluation of the time delay between two or more corrupted versions of a signal received at spatially separated sensors used in positioning, adaptive tracking, speed sensing, direction finding, biomedicine, geophysics, etc. [5]. Delay estimation can be done using the standard least mean squares (LMS) algorithm [6] or the adaptive quadrature delay estimator (QDE) method [7]. Frequency estimation of sinusoidal signals also has applications in adaptive control. For instance, it can be used to estimate the rotating speed of a DVD player [8]. The frequency estimation in this case is done by the use of Notch and funnel filters.

In addition to the practical applications mentioned above, estimation of frequencies and amplitudes of sinusoidal signals buried in additive white noise can be considered as a test procedure for evaluating spectrum analysis techniques. Hence, the spectrum estimation methods are used frequently for estimating frequencies and amplitudes of the sinusoidal signals as well. Periodogram analysis is a classical technique, and despite its disadvantages, it is still used today. Other methods have been also developed which yield better results than the Periodogram, such as autoregressive moving average (ARMA) method, maximum entropy (ME) method, ML method, Pisarenko's method of harmonic retrieval, etc. [9, 10].

1.1 A Review of Methods of Estimation of Sinusoids

As mentioned above, there are different methods for estimating the parameters of the sinusoidal signal. In this section, we briefly review some of the important ones. Least squares (LS) methods are widely used for amplitude estimation. Let the corrupted observation of K complex-valued sinusoids be

$$x[n] = \sum_{l=1}^{K} \alpha_l e^{j\omega_l n} + v[n], \qquad n = 0, 1, \cdots, N-1, \tag{1.1}$$

where α_l is the complex amplitude of the k-th sinusoid, N is the number of available data samples, and $v[n]$ is the observation noise. This can be written in the vector format as

$$\mathbf{x} = \mathbf{A}\boldsymbol{\alpha} + \mathbf{v}, \tag{1.2}$$

where A is an $N \times K$ matrix defined by

$$\mathbf{A} = \begin{bmatrix} 1 & \cdots & 1 \\ e^{j\omega_1} & \cdots & e^{j\omega_K} \\ \vdots & \vdots & \vdots \\ e^{j(N-1)\omega_1} & \cdots & e^{j(N-1)\omega_K} \end{bmatrix}. \tag{1.3}$$

The LS estimate of α is

$$\hat{\boldsymbol{\alpha}} = (\mathbf{A}^H\mathbf{A})^{-1}\mathbf{A}^H\mathbf{x}, \tag{1.4}$$

where $\mathbf{A}^H$ is the conjugate transpose of matrix $\mathbf{A}$. By choosing the estimate as above, the mean squared error is set to minimum. In the WLS method, vector $\mathbf{x}$ is divided into L overlapping subvectors. In MAFI estimators, subvectors of the

observation data are prefiltered in order to yield maximum SNR at filter outputs, and the amplitudes of these filtered subvectors are estimated using the LS or WLS estimators. Then, all these methods can be adjusted to estimate one or K amplitudes at a time.

Quadrature delay estimators are used for time delay estimation using sinusoidal signals. The problem here is to determine the phase delay ϕ between the sinusoids given by

$$\begin{aligned} x_1[n] =& A_1 \cos(2\pi f_0 n) + n_1[n] \\ x_2[n] =& A_2 \cos(2\pi f_0 n + \phi) + n_2[n]. \end{aligned} \tag{1.5}$$

If the frequency of the input signal is known, the quadrature reference signals are generated as

$$\begin{aligned} x_I[n] &= A\cos(2\pi f_0 n) \\ x_Q[n] &= -A\sin(2\pi f_0 n), \end{aligned} \tag{1.6}$$

and are multiplied by both x_1 and x_2 to produce $Q_{m_1}[n]$ and $Q_{m_2}[n]$. Then, the modulated signals are passed through a low pass filter and the phase for each modulated signal is calculated using the following formula

$$\phi = \tan^{-1}\left[\frac{LPF[Q_{m_2}[nT]]}{LPF[Q_{m_1}[nT]]}\right], \tag{1.7}$$

where T is the sampling period. The phase difference is calculated and yields the time delay. If the frequency of the input signal is not known, the quadrature-phase and in-phase signals are generated from x_1 using

$$\begin{aligned} x_{1I}[n] &= x_1[n] = A_1 \cos(2\pi f_0 n) + n_1[n] \\ x_{1Q}[n] &= H[x_1[n]] = A_1 \sin(2\pi f_0 n) + n_3[n], \end{aligned} \tag{1.8}$$

where $H[\,.\,]$ is the Hilbert transform operator. Then x_2 is modulated by x_{1I} and x_{1Q} to form $Q_{m_1}[nT]$ and $Q_{m_2}[nT]$. Adaptive QDE can be obtained by adding an adaptive fractional-delay filter, $h[n,\hat{\phi}]$, into the signal path of x_1 and minimizing $\phi - \hat{\phi}$.

The periodogram method is a classical technique of spectral estimation that is based on the discrete Fourier transform (DFT) of the observed data [11]. The periodogram estimate for a segment of data is defined as the DFT of the sample autocorrelation of the windowed signal

$$\tilde{S}(\omega) = \frac{1}{L} \sum_{m=-(L-1)}^{L-1} c_{vv}[m] e^{-j\omega m}, \tag{1.9}$$

where L is the length of the window and $c_{vv}[m]$ is the autocorrelation of the windowed signal $v[n]$ defined by

$$c_{vv}[m] = \sum_{n=0}^{L-1} v[n]v[n+m]. \tag{1.10}$$

It can also be defined by the moduli of the DFT coefficients of the windowed signal

$$\tilde{S}(\omega_k) = \frac{1}{L}|V[k]|^2. \tag{1.11}$$

The periodogram is not a powerful estimation method because the variance of the estimate exceeds its mean value and the estimate will be biased. Another method based on the DFT operation is the Blackman-Tukey method [12]. The spectral estimation is carried out by estimating the autocorrelation function from the observed data, windowing the autocorrelation estimate, and then obtaining the DFT of the windowed autocorrelation. This method is also known as the moving average (MA) method. Windowing the autocorrelation reduces the bias but the problem of spectral resolution when a short segment of data is available remains because of the effect

of excessive side lobes. Increased resolution can be achieved by averaging the periodogram of the segments of the windowed autocorrelation, or by zero padding the windowed autocorrelation function prior to calculating the DFT.

The ME method, is based on autoregressive modeling of the spectrum. The spectrum estimate is given by fitting an M-th-order autoregressive model to the available autocorrelation segments. This is the same as using a prediction filter to extrapolate the autocorrelation segments, instead of zero padding, in order to minimize the bias. ME method works well specially when a small number of samples are available.

The ML method can be thought as a bank of narrowband filters, each designed to pass a sinewave at the center frequency of the filter and attenuate all other frequencies.

Pisarenko's method finds a polynomial that has zeros on the unit circle at the desired frequencies, to obtain infinite spectral resolution. The desired polynomial can be formed by solving

$$\mathbf{Ra} = \boldsymbol{\lambda}\mathbf{a}, \tag{1.12}$$

where $\mathbf{R}$ is the autocorrelation matrix and $\mathbf{a}$ is the coefficients matrix. Then, the polynomial A(z) can be found by selecting the eigenvector associated with the minimum eigenvalue, and the roots of $A(z)$ give the sinusoids' frequencies. In general Pisarenko's method of spectral estimation yields the best spectral resolution [10].

1.2 The History of Development of Theory of Wirtinger-Type Inequalities

The study of inequalities which involve integrals of functions and their derivatives has a history of about one century. The Wirtinger and Hardy type inequalities are in this category. An example of continuous-time Wirtinger inequality is given below [13,14].

If f is a periodic function with period 2π and $\int_0^{2\pi} f(x)\,dx = 0$ then

$$\int_0^{2\pi} f(x)^2\,dx \leq \int_0^{2\pi} f'(x)^2\,dx, \tag{1.13}$$

satisfying equality in (1.13) if and only if $f(x) = A\cos x + B\sin x$, where A and B are constants.

The applications of these classes of inequalities make them very important in mathematics among other inequalities. Their application extends to applied mathematics, the theory of differential equations, approximation, and probability [15]. An important class of inequalities in this category is ascribed to Wilhelm Witinger. Wirtinger-type inequalities have been generalized and extended in many different directions. It appears that the first analogue of Wirtinger's inequality was given by W. Blaschke [16], and later, discrete versions of Wirtinger-type inequalities were introduced by I.J Schoenberg in 1950 in a paper on finite Fourier series [17]. In 1955, Fan, Taussky, and Todd [13] published a paper in which discrete analogues of the most important Wirtinger-type inequalities were derived. This was followed by a huge interest in the field of discrete inequalities. Later in 1992, G.V. Milovanovic and I.Z. Milovanovic [14] determined the "converse" of the inequalities proved by Fan,

Taussky and Todd.

In 1960, another type of these inequalities was introduced by Zdzidlaw Opial. Although the Opial inequality can be derived from Wirtinger and Hardy type inequalities, its advantage is that it can have the best constant compared to the other types. Many simplifications and improvements have been done on Opial inequalities and generalizations and discrete analogues have been found, making the study of Opial-type inequalities a substantial field with many new and important applications. Specifically, discrete inequalities of Opial type were introduced in 1967-1969 [15]; G.V. Milovanovic and I.Z. Milovanovic [14] and later R.P. Agarwal [15], worked on them. Discrete Wirtinger inequalities are generalized for higher-order differences and two-sided versions are provided in [15] and [14].

1.3 Existing Wirtinger-Type Inequalities

As mentioned in section 1.2, the first discrete inequality of Wirtinger type was given by Schoenberg [17]. In his paper, Schoenberg stated that if $v_0, v_1, \cdots, v_{N-1}$ are the vertices of a N-gon such that $\sum v_n = 0$, and $v'_0, v'_1, \cdots, v'_{N-1}$ being the midpoints of its sides, then

$$\sum_{n=0}^{N-1} |v'_n|^2 \leq \cos^2 \frac{\pi}{N} \sum_{n=0}^{N-1} |v_n|^2, \tag{1.14}$$

and the equality in (1.14) is satisfied if and only if

$$v_n = \zeta_1 W_{s_N} + \zeta_{k-1} \bar{W}_{s_N}, \qquad n = 0, \cdots, N-1, \tag{1.15}$$

He also showed that for cyclic transformation, $v'_n = v_{n+1} - v_n$, the following

inequality holds

$$\sum_{n=0}^{N-1} |v_{n+1} - v_n|^2 \geq 4 \sin^2 \frac{\pi}{N} \sum_{n=0}^{N-1} |v_n|^2. \tag{1.16}$$

However, he only used these results in solutions to geometric problems. In [13], Fan *et al.* proved that for a real sequence $x[1], \cdots, x[N]$, under the conditions that $x[1] = 0$ the following inequality holds

$$\sum_{n=1}^{N-1} (x[n] - x[n+1])^2 \geq 4 \sin^2 \frac{\pi}{2(2N-1)} \sum_{n=2}^{N} x[n]^2, \tag{1.17}$$

with the equality if and only if $x[n] = \hat{x}[n] = A \sin \dfrac{(n-1)\pi}{(2N-1)}$, $n = 1, \cdots, N$, where A is an arbitrary constant.

In addition to similar inequalities as well as some generalizations to the Schoenberg and Fan *et al.* inequalities, Milovanovic and Milovanovic obtained an interesting result in their paper. They introduced a general method for finding the best possible constants A_N and B_N in inequalities

$$A_N \sum_{n=1}^{N} p[n]x[n]^2 \leq \sum_{n=1}^{N} r[n]|x[n] - x[n+1]|^2 \leq B_N \sum_{n=1}^{N} p[n]x[n]^2, \tag{1.18}$$

where $p[n]$ and $r[n]$ are weight sequences and $x[n]$ is an arbitrary sequence of real numbers.

The proofs given in both the papers by Fan *et al.* and Milovanovic and Milovanovic are based on eigenvalues of certain Hermitian matrices. In [18], Lunter gives new proofs for discrete Wirtinger inequalities as well as new generalizations. Lunter and Schoenberg both used Parseval's theorem and circular convolution in their proofs, which is more appropriate in the context of digital signal processing.

1.4 Goals and Contributions of The Thesis

Although a lot of applications have been found for Wirtinger inequalities, little work has been done on them in the context of digital signal processing. In this thesis, we exploit discrete Wirtinger-type inequalities to propose an approach for the estimation of SNR of a single-tone sinusoidal signal buried in white noise. A method has been implemented in which the energy of a signal and the energy of its circular convolution with the impulse response of a filter are calculated in the time domain. By the use of a Wirtinger-type inequality, these two quantities are used to produce a measure of strength at different signal-to-noise ratios. The proposed method is used to estimate the SNR of a sinusoidal signal of a known frequency $\frac{\pi}{N}$ by reading the estimated SNR from the performance curve.

One of the challenges that we faced was to eliminate the conditions that the signals should meet in order to be used in the method. Derivation of the existing Wirtinger inequalities with a digital signal processing approach showed that the equalizing signals of the existing inequalities have constraints in order to be used in real world applications. The constraints, which are the fixed phase and boundary conditions, are removed by expanding the inequalities and modifying them.

For real-world applications, the existing inequalities are not flexible as they do not have any changeable parameter. Consequently, one of our research goals was to generalize these inequalities in order to have an estimation method with enhanced adaptability to different estimation requirements providing multiple filter choices. Generalizations of Wirtinger inequalities are carried out as an attempt to find in-

equalities with better performance curves. The generalized inequalities showed improvement in the performance curves. However, it is a tedious task to find inequalities for higher frequencies other than $\frac{\pi}{N}$.

Another important goal in this thesis is to find a method that is able to estimate the SNR of a sinusoidal signal whose frequency is a rational multiple of π, i.e. $\frac{M}{N}\pi$. It is shown that using a permutation technique and Euclid's algorithm, the observed signal of a rational frequency $\frac{M}{N}\pi$ can be converted to a signal with the frequency $\frac{\pi}{N}$. Then, the SNR of the converted signal can be estimated by the proposed estimation method.

Note that we are not comparing our method to the existing methods of sinusoid estimation. The difference between the method in this thesis and estimation methods is that these methods estimate sinusoidal signal parameters, which is frequency, amplitude and phase, while in our method we are interested in finding the relative strength of the sinusoidal signal in presence of additive white noise.

After all the generalizations and developments, we propose a method for the measurement of signal strength that has the following advantages and features:

(i) It can be applied in the time domain.

(ii) It can be used for any sinusoidal signal whose frequency is a rational multiple of π, and is buried in an additive white noise.

(iii) The computational complexity and, consequently, the cost of implementation is very low.

(iv) The strength of the signal for all frequencies can be measured by a single filter.

(v) Calculation of DFT is not needed.

There are some improvements that can be considered for this method to be applicable to multi-tone signals or in connection with using an optimized filter but those topics are beyond the scope of this thesis and require investigation as future work.

1.5 Organization of the Thesis

In Chapter 2, the existing discrete Wirtinger inequalities are derived using a DFT-based approach. Also a point unnoticed by other authors regarding the existing inequalities is stated. In Chapter 3, we propose a method for estimating the SNR of sinusoids of known frequency $\frac{\pi}{N}$. The modification of the existing inequalities required by this method is done and the proposed method is simulated using MATLAB R2006a, for the modified inequalities. The performance curves are obtained result. In Chapter 4, generalizations of these methods to weighted inequalities are provided and the performance curves at different weights for each inequality are analyzed. In Chapter 5, we study estimation of the SNR of sinusoids of frequency $\frac{M}{N}\pi$ and propose a solution by a combination of signal reordering and modulation to convert the sinusoid of frequency $\frac{M}{N}\pi$ to the form of a sinusoid containing frequency $\frac{\pi}{N}$. The solution is based on a permutation property and Euclid's algorithm. The process of estimation of the SNR of sinusoids with arbitrary rational frequencies $\frac{M}{N}\pi$ is detailed. The optimal values of the weights for inequalities with two weights are obtained and the computational complexity of the proposed method is analyzed. We also study the case where the available samples are fewer than the minimum required. Numerical

results show that the method is still capable of estimating the SNR in such cases. Finally, in Chapter 6, advantages of the method are discussed and a possible industrial application of the method is described.

Chapter 2

Derivation of Existing Discrete-Time Wirtinger Inequalities Using a DFT-Based Approach

Our objective in this chapter is to restate some inequalities of Fan *et al.* [13], and Milovanovic and Milovanovic [14] that will be used in Chapter 3 in digital signal processing context. To be self contained, the proof is thoroughly explained. The original proofs can be found in [18].

As mentioned in the previous chapter, Fan *et al.* [13] and Milovanovic and Milovanovic [14] used a Hermitian matrix to prove the inequalities, while, Lunter [18] and Schoenberg [17] used Parseval's theorem and circular convolution in their proofs. In

this chapter, we rephrase the proof given by Lunter in [18], but the difference here is that we are deriving these inequalities in the context of digital signal processing. We provide details of the derivation steps for one of the inequalities and then follow the same approach for the other inequalities. We carry out a new result and propose it as a remark for one of the inequalities.

2.1 Preliminary

2.1.1 DFT and Circular Convolution

We use the notation $x[n]$, $n = 0, 1, \cdots, N-1$, to denote a discrete-time signal where N is the length. The DFT is defined as

$$X[k] = \sum_{n=0}^{N-1} x[n] W_N^{kn}, \qquad 0 \leq k \leq N-1, \tag{2.1}$$

where $W_N = e^{-j(2\pi/N)}$. The inverse discrete Fourier transform is given by

$$x[n] = \frac{1}{N} \sum_{k=0}^{N-1} X[k] W_N^{-kn}, \qquad 0 \leq n \leq N-1. \tag{2.2}$$

The relationship between $x[n]$ and $X[k]$ is written as $x[n] \overset{\mathcal{DFT}}{\longleftrightarrow} X[k]$. If we define the squared norm of $x[n]$ as

$$\|x[n]\|^2 = \sum_{n=0}^{N-1} |x[n]|^2, \tag{2.3}$$

then, due to Parseval's theorem

$$\sum_{n=0}^{N-1} |x[n]|^2 = \frac{1}{N} \sum_{k=0}^{N-1} |X[k]|^2. \tag{2.4}$$

We can write

$$\|X[k]\|^2 = N \|x[n]\|^2. \tag{2.5}$$

This means that DFT only changes the norm of the signal by factor N. This is very useful since it is sometimes easier to calculate the norm in the other domain.

It can be shown that the response of any LTI system to an input can be expressed by the linear convolution of the input signal with the impulse response of the system in the time domain [11]. In the case of finite length signals, we can use the circular convolution to find the output of the system after a proper zero padding. Let $x_3[n]$ be the circular convolution of two signals $x_1[n]$ and $x_2[n]$, both of length N, and with DFTs $X_1[k]$ and $X_2[k]$, respectively. Then we have

$$\begin{aligned} x_3[n] &= x_1[n] \textcircled{N} x_2[n] \\ &= \sum_{m=0}^{N-1} x_2[m] x_1[((n-m))_N], \end{aligned} \tag{2.6}$$

where $((n-m))_N$ is the value of $n-m$ modulo N. Expanding (2.6) gives the following

$$\begin{aligned} x_3[0] =& x_2[0]x_1[0] + x_2[1]x_1[N-1] + \cdots + x_2[N-1]x_1[1] \\ x_3[1] =& x_2[0]x_1[1] + x_2[1]x_1[0] + \cdots + x_2[N-1]x_1[2] \\ &\vdots \\ x_3[N-1] =& x_2[0]x_1[N-1] + x_2[1]x_1[N-2] + \cdots + x_2[N-1]x_1[0]. \end{aligned} \tag{2.7}$$

In the frequency domain, we can write

$$X_3[k] = X_1[k]X_2[k]. \tag{2.8}$$

2.1.2 Forward Difference Systems

The first-order forward difference system is defined by the input-output relationship

$$y^{(1)}[n] = x[n+1] - x[n]. \tag{2.9}$$

The second-order forward difference is defined by

$$y^{(2)}[n] = y^{(1)}[n+1] - y^{(1)}[n] = x[n] - 2x[n+1] + x[n+2], \tag{2.10}$$

and by induction, the following expansion can be obtained

$$y^{(m)}[n] = \sum_{p=0}^{m} (-1)^{m-p} \binom{m}{p} x[n+p]. \tag{2.11}$$

The forward difference system can also be represented by its impulse response. Let $h_f[n]$ be the impulse response of the first order forward difference system. After a proper zero padding, the output $y^{(1)}[n]$ can be expressed as the circular convolution of the input $x[n]$ and the impulse response $h_f[n]$, both with length N, given by

$$h_f[n] = \begin{cases} -1, & n = 0 \\ 1, & n = N-1 \\ 0, & \text{otherwise.} \end{cases} \tag{2.12}$$

To find the input-output relationship in the frequency domain, we first obtain the N-point DFT of the impulse response

$$H_f[k] = \sum_{n=0}^{N-1} h_f[n] W_N^{kn} = e^{j(2\pi/N)k} - 1, \qquad 0 \le k \le N-1. \tag{2.13}$$

The moduli are given by

$$|e^{j(2\pi/N)k} - 1|^2 = 2 - 2\cos\frac{2\pi k}{N}, \qquad 0 \le k \le N-1, \tag{2.14}$$

and we can write

$$|Y[k]|^2 = |H_f[k]X[k]|^2, \tag{2.15}$$

or

$$\sum_{k=0}^{N-1} |Y[k]|^2 = \sum_{k=0}^{N-1} |H_f[k]X[k]|^2. \tag{2.16}$$

Applying Parseval's theorem to the left side of (2.16), we get

$$N\sum_{n=0}^{N-1}|y[n]|^2=\sum_{k=0}^{N-1}|H_f[k]|^2|X[k]|^2. \tag{2.17}$$

Substituting (2.14) in (2.17) results

$$N\sum_{n=0}^{N-1}|y[n]|^2=\sum_{k=0}^{N-1}\Big(2-2\cos\frac{2\pi k}{N}\Big)|X[k]|^2, \tag{2.18}$$

and, by induction, for an m^{th}-order forward difference system the following applies

$$N\sum_{n=0}^{N-1}|y^{(m)}[n]|^2=\sum_{k=0}^{N-1}\Big(2-2\cos\frac{2\pi k}{N}\Big)^m|X[k]|^2. \tag{2.19}$$

In the next section, we derive propositions based on the properties of (2.18). We take this equation as the core of every inequality in this thesis.

2.2 Propositions of Wirtinger-Type Inequalities and Their Proofs

We now rephrase some fundamental propositions given in [18] and provide their proofs in the digital signal processing context.

Proposition 1 *Consider a signal $x[n]\in\mathbb{C}^N$, where $\mathbb{C}^N$ is the N-dimensional complex space. Let $m\in\mathbb{N}$ be a positive integer. Then the following statements hold.*

(a) If $\sum_{n=0}^{N-1}x[n]=0$, then

$$\|y^{(m)}[n]\|^2\geq\Big(2-2\cos\frac{2\pi}{N}\Big)^m\|x[n]\|^2, \tag{2.20}$$

with equality if and only if $x[n] = \alpha e^{j(2\pi/N)k} + \beta e^{-j(2\pi/N)k}$, *where* α *and* β *are complex constants in* $\mathbb{C}$.

(b) If N *is even, and* $\sum_{n=0}^{N-1}(-1)^n x[n] = 0$, *then*

$$\|y^{(m)}[n]\|^2 \leq \left(2 + 2\cos\frac{2\pi}{N}\right)^m \|x[n]\|^2, \tag{2.21}$$

with equality if and only if $x[n] = \alpha e^{j(2\pi/N)(N/2+1)n} + \beta e^{j(2\pi/N)(N/2-1)n}$, *where* $\alpha, \beta \in \mathbb{C}$.

(c) If N *is even, and* $\sum_{n=0}^{N-1} e^{j(2\pi/N)ln} x[n] = 0$ *for* $l = \frac{1}{2}N$, $\frac{1}{2}N - 1$, *and* $\frac{1}{2}N + 1$, *then*

$$\|y^{(m)}[n]\|^2 \leq \left(2 + 2\cos\frac{4\pi}{N}\right)^m \|x[n]\|^2, \tag{2.22}$$

with equality if and only if $x[n] = \alpha e^{j(2\pi/N)(N/2+2)n} + \beta e^{j(2\pi/N)(N/2-2)n}$, *where* $\alpha, \beta \in \mathbb{C}$.

Proof.

(a) Assume that $\|x[n]\|^2$ is held constant. This is the same as keeping $\sum_{k=0}^{N-1} |X[k]|^2$ constant. The assumption $\sum_{n=0}^{N-1} x[n] = 0$ in part (a) is equivalent to

$$X[0] = 0. \tag{2.23}$$

Now we can write (2.19) in the form of

$$N\sum_{n=0}^{N-1} |y^{(m)}[n]|^2 \geq \min_{\substack{k=0,\cdots,N-1 \\ X[0]=0}} \left\{(2 - 2\cos\frac{2\pi k}{N})^m\right\}\left(\sum_{k=0}^{N-1} |X[k]|^2\right). \tag{2.24}$$

This inequality holds because $(2 - 2\cos\frac{2\pi k}{N})$ is a factor independent of the DFT coefficients $X[k]$. The minimum of $(2 - 2\cos\frac{2\pi k}{N})$ is zero and is attained at $k = 0$,

by the assumption, $X[0] = 0$. The next smallest value is obtained at $k = 1$ or $k = N - 1$

$$\min_{k=1,\cdots,N-1} \left(2 - 2\cos\frac{2\pi k}{N}\right)^m = \left(2 - 2\cos\frac{2\pi}{N}\right)^m. \tag{2.25}$$

Therefore, we can write

$$N\sum_{n=0}^{N-1} |y^{(m)}[n]|^2 \geq \left(2 - 2\cos\frac{2\pi}{N}\right)^m \sum_{k=0}^{N-1} |X[k]|^2, \tag{2.26}$$

and by using Parseval's theorem (2.4) we have

$$\sum_{n=0}^{N-1} |y^{(m)}[n]|^2 \geq \left(2 - 2\cos\frac{2\pi}{N}\right)^m \sum_{n=0}^{N-1} |x[n]|^2. \tag{2.27}$$

Now we want to determine the signal which renders an equality. To do this, we should find the minimum of $\sum_{n=0}^{N-1} |y^{(m)}[n]|^2$ under the assumption that $\sum_{n=0}^{N-1} |x[n]|^2$ is held constant. Letting $\sum_{n=0}^{N-1} |x[n]|^2 = \epsilon$, we have

$$\min_{\substack{X[0]=0 \\ \sum_{k=0}^{N-1} |X[k]|^2 = \epsilon}} \sum_{n=0}^{N-1} |y^{(m)}[n]|^2 = \min_{\substack{X[0]=0 \\ \sum_{k=0}^{N-1} |X[k]|^2 = \epsilon}} \sum_{k=0}^{N-1} \left(2 - 2\cos\frac{2\pi k}{N}\right)^m |X[k]|^2. \tag{2.28}$$

In view of (2.26), the minimum is bounded by the product of the minimum of $(2 - 2\cos\frac{2\pi k}{N})^m$ and $\sum_{k=0}^{N-1} |X[k]|^2$. If the DFT of $x[n]$ only has the coefficients at the index k that produces the least factor associated to it, then that signal will produce the minimum of $\sum_{n=0}^{N-1} |y^{(m)}[n]|^2$. As we can see in Fig. 2.1, the minimum of $(2 - 2\cos\frac{2\pi k}{N})^m$ is zero but since $X[0] = 0$, the minimum in (2.28) is attained if and only if the DFT coefficients, $X[k]$, are zero for all k except for $k = 1$ and $k = N - 1$. Hence the minimizing signal is

$$X[k] = \begin{cases} \alpha, & k = 1 \\ \beta, & k = N - 1 \\ 0, & \text{otherwise,} \end{cases} \tag{2.29}$$

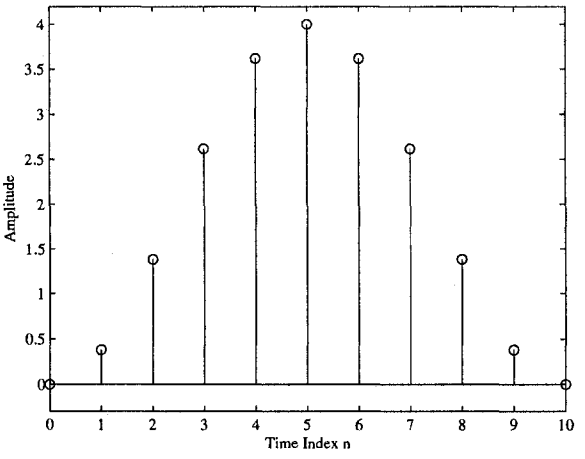

Figure 2.1: $2 - 2\cos(2\pi k/N)$ for $N = 10$.

or, equivalently

$$x[n] = \alpha e^{j(2\pi/N)n} + \beta e^{-j(2\pi/N)n}, \qquad \alpha, \beta \in \mathbb{C}. \tag{2.30}$$

(b) In this case, N is even, but we have $\sum_{k=0}^{N-1}(-1)^n x[n] = 0$, which means

$$X[k]\big|_{k=N/2} = 0. \tag{2.31}$$

Hence the next largest value is attained when $k = \frac{N}{2} \pm 1$, and is equal to

$$\left(2 - 2\cos\frac{2\pi k}{N}\right)\Big|_{k=\frac{N}{2}\pm 1} = 2 + 2\cos\frac{2\pi}{N}, \tag{2.32}$$

whereby the inequality is proved, and the signal for which the equality holds is

$$x[n] = \alpha e^{j(2\pi/N)(N/2+1)n} + \beta e^{j(2\pi/N)(N/2-1)n}, \qquad \alpha, \beta \in \mathbb{C}. \tag{2.33}$$

(c) This case is almost the same as part (b), but here the DFT coefficients at $k = \frac{N}{2}+1$ and $k = \frac{N}{2} - 1$ are also zero. Consequently, the maximum is obtained when

$k = \frac{N}{2} \pm 2$. It follows that

$$\Big(2 - 2\cos\frac{2\pi k}{N}\Big)\Big|_{k=\frac{N}{2}\pm 2} = 2 + 2\cos\frac{4\pi}{N}, \tag{2.34}$$

which leads to the equality and the corresponding equalizing signal.

2.3 Derivation of Existing Discrete-Time Wirtinger Inequalities

The following inequalities were given by Fan *et al.* [13].

(1) If $x[1], \cdots, x[N-1]$ are real numbers, and $x[0] = x[N] = 0$, then

$$\sum_{n=0}^{N-1}(x[n+1] - x[n])^2 \geq 2\Big(1 - \cos\frac{\pi}{N}\Big)\sum_{n=0}^{N-1} x[n]^2, \tag{2.35}$$

with equality if and only if $x[n] = \hat{x}[n] = A\sin\big(\pi n/N\big)$, where A is a real constant.

(2) If $x[1], \cdots, x[N-1]$ are real and $x[0] = 0$, then

$$\sum_{n=0}^{N-2}(x[n+1] - x[n])^2 \geq 2\Big(1 - \cos\frac{\pi}{2N-1}\Big)\sum_{n=0}^{N-1} x[n]^2, \tag{2.36}$$

with equality if and only if $x[n] = \hat{x}[n] = A\sin\big(\pi n/(2N-1)\big)$, $n = 1, \cdots, N-1$, where A is a real constant.

The next two inequalities, were found by Milovanovic and Milovanovic [14].

(3) If $x[1], \cdots, x[N-1]$ are real numbers, and $x[0] = x[N] = 0$, then

$$\sum_{n=0}^{N-1}(x[n+1] - x[n])^2 \leq 2\Big(1 + \cos\frac{\pi}{N}\Big)\sum_{n=0}^{N-1} x[n]^2, \tag{2.37}$$

with equality if and only if $x[n] = \hat{x}[n] = A(-1)^n\sin\big(\pi n/N\big)$, $n = 1, \cdots, N-1$, where A is a real constant.

(4) If $x[1], \cdots, x[N-1]$ are real and $x[0] = 0$, then

$$\sum_{n=0}^{N-2}(x[n+1]-x[n])^2 \leq 2\Big(1+\cos\frac{\pi}{2N-1}\Big)\sum_{n=0}^{N-1}x[n]^2, \tag{2.38}$$

with equality if and only if $x[n] = \hat{x}[n] = A(-1)^n \sin\big(2\pi n/(2N-1)\big)$, $n = 1, \cdots, N-1$.

The structure of the proofs for all the inequalities (but one) is the same [18], but we restate the proofs using a DFT-based approach. Let $x[n] \in \mathbb{R}^N$ be a real signal satisfying the boundary conditions stated in the inequality we want to prove. We embed this signal in $\mathbb{C}^M$ as a complex periodic signal $v[i]$, $M > N$. The embedding process is performed so that $\sum_i |v[i]|^2$ is a multiple of $\sum_n |x[n]|^2$, and also $\sum_i |v[i+1]-v[i]|^2$ is a multiple of $\sum_n |x[n+1]-x[n]|^2$. We apply Proposition 1 to the embedded signal $v[i]$. The embedding should be done in such a way that the embedded signal $v[i]$ satisfies the conditions in the corresponding part of the proposition. Finally, we look for an embedded real signal which has the form of the signal we started with, i.e., $x[n]$. Since $\sum_n |x[n+1]-x[n]|^2$ and $\sum_n |x[n]|^2$ are multiples of the norms of the corresponding complex signals, the real signal $x[n]$ minimizes (or maximizes) $\sum_n |x[n+1]-x[n]|^2$ under a fixed $\sum_n |x[n]|^2$.

All the proofs for the inequalities are based on the following important points.

- All the inequalities in this chapter are based on (2.18).
- We use embedding in order to satisfy the conditions in Proposition 1.
- The conditions in Proposition 1 are used to determine which Fourier components form the equalizing signal.

Proof.

(1) Embed the real finite signal $x[n] \in \mathbb{R}^N, n = 0, \cdots, N-1$ in $\mathbb{C}^{2N}$ as follows

$$v[i]\Big|_{i=0:2N-1} = \big(x[0], x[1], \cdots, x[N-1], -x[0], -x[1], \cdots, -x[N-1]\big). \quad (2.39)$$

This type of embedding satisfies the condition $\sum_{i=0}^{2N-1} v[i] = 0$ required in Proposition 1(a). Applying proposition 1 to $v[i]$ with $m = 1$, we have

$$\sum_{i=0}^{2N-1} (v[i+1] - v[i])^2 \geq \Big(2 - 2\cos\frac{\pi}{N}\Big) \sum_{i=0}^{2N-1} v[i]^2. \quad (2.40)$$

Now the right side can be written as

$$\sum_{i=0}^{2N-1} v[i]^2 = 2\sum_{n=0}^{N-1} x[n]^2, \quad (2.41)$$

and for the left side

$$\begin{aligned}
&\sum_{i=0}^{2N-1} (v[i+1] - v[i])^2 = (x[1] - x[0])^2 + (x[2] - x[1])^2 + \cdots \\
&+ (x[N-1] - x[N-2])^2 + (-x[0] - x[N-1])^2 + (-x[1] + x[0])^2 \\
&+ (-x[2] + x[1])^2 + \cdots + (-x[N-1] + x[N-2])^2 + (x[0] + x[N-1])^2.
\end{aligned} \quad (2.42)$$

If we calculate the sum on $x[n]$ we obtain

$$\begin{aligned}
\sum_{n=0}^{N-1} (x[n+1] - x[n])^2 &= (x[1] - x[0])^2 + (x[2] - x[1])^2 \\
&+ \cdots + (x[N-1] - x[N-2])^2 + (x[0] - x[N-1])^2.
\end{aligned} \quad (2.43)$$

Comparing (2.43) and (2.42), in order for $\sum_{i=0}^{2N-1}(v[i+1]-v[i])^2$ to be proportional to $\sum_{n=0}^{N-1}(x[n+1] - x[n])^2$, we should have

$$(x[0] + x[N-1])^2 = (x[0] - x[N-1])^2, \quad (2.44)$$

or

$$x[0]x[N-1] = -x[0]x[N-1]. \tag{2.45}$$

Equivalently either $x[0] = 0$ or $x[N-1] = 0$. In either case we will have

$$\sum_{i=0}^{2N-1} (v[i+1] - v[i])^2 = 2\sum_{n=0}^{N-1} (x[n+1] - x[n])^2. \tag{2.46}$$

Hence, (2.40) leads us to the inequality

$$\sum_{n=0}^{N-1} (x[n+1] - x[n])^2 \geq \left(2 - 2\cos\frac{\pi}{N}\right) \sum_{n=0}^{N-1} x[n]^2. \tag{2.47}$$

To determine the real signal that yields an equality, we must find among the signals that minimize the left hand side, the one that is created by embedding a real signal $x[n]$ in $\mathbb{C}^{2N}$. It is clear that the result of embedding a real signal is a real signal. According to part (a) of Proposition 1, the minimizing signals are of the form $\alpha e^{j(2\pi n)/(2N)} + \beta e^{-j(2\pi n)/(2N)}$. For a real signal of this form the following equality should hold

$$\left(\alpha e^{j(2\pi n)/(2N)} + \beta e^{-j(2\pi n)/(2N)}\right)^* = \alpha e^{j(2\pi n)/(2N)} + \beta e^{-j(2\pi n)/(2N)}, \tag{2.48}$$

or equivalently

$$|\alpha|\left(e^{-j(\frac{2\pi n}{2N}+\theta_\alpha)} - e^{j(\frac{2\pi n}{2N}+\theta_\alpha)}\right) + |\beta|\left(e^{j(\frac{2\pi n}{2N}-\theta_\beta)} - e^{-j(\frac{2\pi n}{2N}-\theta_\beta)}\right) = 0, \tag{2.49}$$

and consequently

$$\sin\frac{2\pi n}{2N}\left(|\alpha|\cos\theta_\alpha - |\beta|\cos\theta_\beta\right) + \cos\frac{2\pi n}{2N}\left(|\alpha|\sin\theta_\alpha + |\beta|\sin\theta_\beta\right) = 0. \tag{2.50}$$

In order for the above equality to hold for all n we must have

$$\begin{cases} |\alpha|\cos\theta_\alpha - |\beta|\cos\theta_\beta = 0 \\ |\alpha|\sin\theta_\alpha + |\beta|\sin\theta_\beta = 0, \end{cases} \tag{2.51}$$

and for the above equations to have a nonzero solution we must have

$$\det \begin{pmatrix} \cos\theta_\alpha & -\cos\theta_\beta \\ \sin\theta_\alpha & \sin\theta_\beta \end{pmatrix} = 0, \tag{2.52}$$

which leads to $\theta_\alpha = -\theta_\beta$, and consequently $|\alpha| = |\beta|$, which together imply $\alpha = \beta^*$. Therefore, the real-valued equalizing signal is

$$\begin{aligned} x[n] = \hat{x}[n] &= \left(|\alpha| e^{j(\pi n/N + \theta_\alpha)} + |\alpha| e^{j(-\pi n/N - \theta_\alpha)}\right) \\ &= 2|\alpha| \cos\left(\frac{\pi n}{N} + \theta_\alpha\right), \end{aligned} \tag{2.53}$$

or

$$\hat{x}[n] = A\cos\left(\frac{\pi n}{N} + \gamma\right), \qquad A, \gamma \in \mathbb{R}. \tag{2.54}$$

Now two cases exist.

(i) $x[0] = 0$. This implies that for the equalizing signal $\hat{x}[n]$ γ should be $\pi/2$. Hence

$$\hat{x}[n] = A\sin\left(\frac{\pi n}{N}\right). \tag{2.55}$$

In other words, the minimizing signal, $\hat{v}[i]$, is obtained by embedding the real signal $\hat{x}[n] = A\sin(\pi n/N)$. This proves inequality (1).

(ii) $x[N-1] = 0$. In this case, for the inequality to be true, we should have

$$\hat{x}[N-1] = A\cos(\pi(N-1)/N + \gamma) = 0. \tag{2.56}$$

Therefore $\gamma = -\pi/2 + \pi/N$, and the equalizing signal is

$$\hat{x}[n] = A\sin\left(\frac{\pi n}{N} + \frac{\pi}{N}\right). \tag{2.57}$$

This is a new result, not given in [18], that we have obtained for the equalizing signal of inequality (1). We state it here as a remark.

Remark 1 *If* $x[1], \cdots, x[N-1]$ *are real numbers, and* $x[N-1] = 0$, *then*

$$\sum_{n=0}^{N-1}(x[n+1] - x[n])^2 \geq \left(2 - 2\cos\frac{\pi}{N}\right)\sum_{n=0}^{N-1} x[n]^2, \tag{2.58}$$

with equality if and only if $x[n] = \hat{x}[n] = A\sin(\pi n/N + \pi/N)$, *where* A *is a real constant.*

Note that inequality (1) turns to an equality not only when $x[n] = A\sin\left(\frac{\pi n}{N}\right)$ but also when $x[n] = A\sin\left(\frac{\pi n}{N} + \frac{\pi}{N}\right)$. This means that the equalizing signal can be written in the form $\hat{x}[n] = A\sin\left(\frac{\pi n}{N} + \gamma\right)$, where $\gamma = 0$ if $x[0] = 0$, or $\gamma = \frac{\pi}{N}$ when $x[N-1] = 0$.

(2) To prove this part, we use inequality (1). First, we embed the real signal $x[n]$ in $q[i]$ so that we can employ the first inequality. The components of $q[i]$ are given by

$$q[i]\Big|_{i=0:2N-1} = \big(x[0], x[1], \cdots, x[N-1], x[N-1], \cdots, x[1], x[0]\big), \tag{2.59}$$

where $x[0] = 0$. It can be shown that

$$\sum_{i=0}^{2N-2}(q[i+1] - q[i])^2 = 2\sum_{n=0}^{N-2}(x[n+1] - x[n])^2, \tag{2.60}$$

because

$$q[N] - q[N-1] = x[N-1] - x[N-1] = 0, \tag{2.61}$$

and it is clear also that

$$\sum_{i=0}^{2N-2} q[i]^2 = 2\sum_{n=0}^{N-1} x[n]^2. \tag{2.62}$$

Since we have $q[0] = q[2N-1] = 0$, inequality (1) applies and

$$\sum_{i=0}^{2N-2}(q[i+1] - q[i])^2 \geq \left(2 - 2\cos\frac{\pi}{2N-1}\right)\sum_{i=0}^{2N-2} q[i]^2. \tag{2.63}$$

This inequality is true because all the conditions required in inequality (1) are satisfied. The only difference is the length of the signal which is $2N-1$ instead of N. Therefore

$$\sum_{n=0}^{N-2}(x[n+1]-x[n])^2 \geq \left(2-2\cos\frac{\pi}{2N-1}\right)\sum_{n=0}^{N-1}x[n]^2. \tag{2.64}$$

Since $x[0]$ must be zero, case (i) applies and the maximizing signals are of the form $\hat{v}[i] = A\sin\big(\pi i/(2N-1)\big)$. For this signal $\hat{v}[N-1-i] = \hat{v}[N+i]$ which shows that it is consistent with the embedding conditions. Thus $\hat{x}[n] = A\sin\big(\pi n/(2N-1)\big)$, where $n = 0, \cdots, N-1$. This proves inequality (2).

(3) The signal we want to embed here is $x[n]$ and $x[0] = x[N] = 0$. We embed this signal in $\mathbb{C}^{2N+2}$ in such a way that

$$\begin{aligned} v[i]\Big|_{i=0:2N-1} =& \big(x[0], x[1], \cdots, x[N-1], \\ & (-1)^{N-1}x[0], (-1)^{N-1}x[1], \cdots, (-1)^{N-1}x[N-1]\big). \end{aligned} \tag{2.65}$$

This implies that $\sum_{i=0}^{2N-1}(-1)^i v[i] = 0$, which satisfies the condition in part (b) of Proposition 1, and we have

$$\sum_{i=0}^{2N-1}(v[i+1]-v[i])^2 \leq \left(2+2\cos\frac{2\pi}{2N}\right)\sum_{i=0}^{2N-1}v[i]^2. \tag{2.66}$$

It is clear that

$$\sum_{i=0}^{2N-1}(v[i+1]-v[i])^2 = 2\sum_{n=0}^{N-1}(x[n+1]-x[n])^2, \tag{2.67}$$

because $x[0] = 0$. Also, it can be easily shown that

$$\sum_{i=0}^{2N-1}v[i]^2 = 2\sum_{n=0}^{N-1}x[n]^2. \tag{2.68}$$

Consequently

$$\sum_{n=0}^{N-1}(x[n+1]-x[n])^2 \leq \left(2+2\cos\frac{\pi}{N}\right)\sum_{n=0}^{N-1}x[n]^2. \tag{2.69}$$

The equality holds if and only if

$$v[i] = \alpha e^{j(2\pi/(2N))((2N)/2+1)i} + \beta e^{j(2\pi/(2N))((2N)/2-1)i}. \tag{2.70}$$

We are looking for a real signal of this form, hence, the imaginary part of this signal should be zero, i.e.,

$$|\alpha|\sin\left(\frac{\pi(N+1)}{N}i+\theta_\alpha\right)+|\beta|\sin\left(\frac{\pi(N-1)}{N}i+\theta_\beta\right)=0, \tag{2.71}$$

or equivalently

$$|\alpha|\cos(\pi i)\sin\left(\frac{\pi i}{N}+\theta_\alpha\right)-|\beta|\cos(\pi i)\sin\left(\frac{\pi i}{N}-\theta_\beta\right)=0 \tag{2.72}$$

For this to be true, we should have $|\alpha|=|\beta|$ and $\theta_\alpha=-\theta_\beta$, which means $\alpha=\beta^*$, and the minimizing real signal is

$$v[i] = A(-1)^i\cos\left(\pi i/N+\gamma\right). \tag{2.73}$$

Since $v[0]=0$, we should have $\gamma=(2m+1)\pi/2$, $m=0,\pm1,\pm2,\ldots$ Therefore our equalizing signal is $v[i]=A(-1)^i\sin\left(\pi i/N\right)$, and is obtained by embedding the real signal $x[n]=A(-1)^n\sin\left(\pi n/N\right)$, $n=0,\cdots,N-1$. This proves inequality (3).

(4) Let $x[1],\cdots,x[N-1]$ be real numbers and $x[0]=0$. We embed this signal in $\mathbb{C}^{4N-2}$ as

$$\begin{aligned} v[i]\Big|_{i=0:4N-2} = \big(&x[0],x[1],\cdots,x[N-1],x[N-1],x[N-2],\cdots,x[1],\\ &-x[0],-x[1],\cdots,-x[N-1],-x[N-1],-x[N-2],\cdots,-x[1]\big). \end{aligned} \tag{2.74}$$

It can be shown that $\sum_{i=0}^{4N-3}(-1)^i v[i] = 0$, because the first quarter of $v[i]$ cancels the second, and the third quarter cancels the fourth. In addition

$$V[k]\big|_{k=(4N-2)/2\pm 1} = \sum_{i=0}^{4N-3}(-1)^i e^{\pm(j2\pi/(4N-2))i} v[i] = 0, \tag{2.75}$$

because we have $v[i] = -v[i+2N-1]$, and the following equality holds

$$\begin{aligned} &v[i](-1)^i e^{\pm(j2\pi/(4N-2))i} + v[i+2N-1](-1)^{i+2N-1} e^{\pm(j2\pi/(4N-2))(i+2N-1)} \\ &= v[i](-1)^i e^{\pm(j2\pi/(4N-2))i} + v[i+2N-1](-1)^i e^{\pm(j2\pi/(4N-2))i} = 0. \end{aligned} \tag{2.76}$$

Thus, all the conditions of part (c) of Proposition 1 are satisfied and we have

$$\sum_{n=0}^{4N-3}(v[i+1]-v[i])^2 \le \left(2+2\cos\frac{4\pi}{4N-2}\right)\sum_{i=0}^{4N-3} v[i]^2. \tag{2.77}$$

Note that

$$\sum_{i=0}^{4N-3}(v[i+1]-v[i])^2 = 4\sum_{n=0}^{N-2}(x[n+1]-x[n])^2, \tag{2.78}$$

because $v[N-1] = v[N]$ and $v[2N-1] = x[0] = -x[0] = 0$. It is also obvious that

$$\sum_{i=0}^{4N-3} v[i]^2 = 4\sum_{n=0}^{N-1} x[n]^2. \tag{2.79}$$

Therefore

$$\sum_{n=0}^{N-2}(x[n+1]-x[n])^2 \le \left(2+2\cos\frac{2\pi}{2N-1}\right)\sum_{n=0}^{N-1} x[n]^2. \tag{2.80}$$

The equality holds if and only if

$$v[i] = \alpha e^{j(2\pi/(4N-2))((4N-2)/2+2)i} + \beta e^{j(2\pi/(4N-2))((4N-2)/2-2)i}. \tag{2.81}$$

The real signals can be found by enforcing $\alpha = \beta^*$ as in inequality (3), and are of the form $v[i] = A(-1)^i \cos\left(2\pi i/(2N-1)+\gamma\right)$. The condition in the inequality (4)

requires that $v[0] = 0$, which yields $\gamma = (2m+1)\pi/2$, $m = 0, \pm 1, \pm 2, \ldots$ Therefore the minimizing signal is $\hat{v}[i] = A(-1)^i \sin\big(2\pi i/(2N-1)\big)$. This signal can be created by embedding the real-valued signal $\hat{x}[n] = A(-1)^n \sin\big(2\pi n/(2N-1)\big)$, $n = 0, \cdots, N-1$, which proves inequality (4).

In the next chapter, we describe how these inequalities give rise to a method for estimating the SNR of a sinusoidal signal with a known frequency.

Chapter 3

Modification of Inequalities and Their Application to Estimation of SNR of Sinusoids

In this chapter, we first propose a method for estimating the SNR of a sinusoidal signal buried in noise using the discrete-time Wirtinger inequalities. The proposed method is based on the notion of average performance curves corresponding to the equalizing sinusoids associated with the inequalities. It is shown how the curves are obtained and how they are used to provide an estimate for the SNR of a sinusoid of fixed length and known frequency. Further, we modify the existing inequalities of Chapter 2 to remove the accompanying constraints and conditions so that they can be used freely in the proposed SNR estimation method. Finally, we provide some simulation results.

3.1 Method of SNR Estimation of Sinusoidal Signals

In the preceding chapter, we derived the existing discrete-time Wiritnger inequalities using a DFT-based approach. In this section, we propose a simple method for estimating the SNR of sinusoids buried in additive white noise using the discrete-time Wirtinger inequalities. We start by noting that the left side of each inequality can be interpreted as the energy of the output of a forward difference system. The right side of the inequalities consists of a constant factor, which depends on the length of the signal, and the energy of the signal $\sum_n x[n]^2$. If the input signal is exactly equal to the equalizing signal of the inequality, it becomes an equality. Thus, we expect that the closer the input gets to the equalizing sinusoid, the closer the two sides of the inequality get in their values. Based on this argument, the closeness between the two sides of the inequality, or the strength of the equalizing sinusoidal signal, can be measured as a ratio. We use this ratio to estimate the SNR of a noisy signal. The ratio is obtained by dividing the two sides of the inequality in a manner that it does not exceed 1. It becomes 1 if and only if the signal is an equalizing signal.

Formally stated, the problem we are concerned with is as follows.

Problem. Estimate the SNR of a finite-length signal, containing a sinusoid of frequency $\frac{\pi}{N}$ and arbitrary phase γ, corrupted with additive white noise.

Note that the fixed value for the frequency of the sinusoid arises from the boundary conditions and other constraints in the existing discrete-time inequalities. The method proposed in this chapter for the solution of the above problem is depicted in

the form of a block diagram in Fig. 3.1.

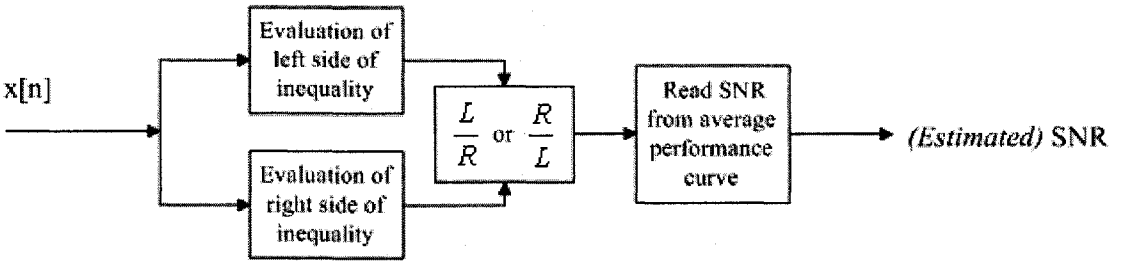

Figure 3.1: Block diagram of the proposed method for estimation of the SNR of a sinusoidal signal with known frequency.

As can be seen in the above diagram, the final step of the SNR estimation method involves reading the SNR value from what we call the average performance curve. The following procedure details how the curve is obtained.

1. A zero mean white noise sequence of the same size as the sinusoid is generated.

2. At each SNR value, the noise is multiplied by an attenuation factor α which is defined as

$$\alpha = \sqrt{10^{-(SNR/10)}} \frac{\sum_{n=0}^{N-1} \hat{x}[n]^2}{\sigma_0^2}, \tag{3.1}$$

   where σ_0^2 is the variance of the noise sequence and $\hat{x}[n]$ is the pure sinusoid.

3. The disturbance $e[n]$ is formed by multiplication of α and the white noise.

4. The observed signal, $x[n]$, is formed by the sum of the sinusoid, $\hat{x}[n] = A\cos(\pi n/N + \gamma)$, $n = 0 : N-1$, and the disturbance $e[n]$.

5. The left and right side of a discrete Wirtinger-type inequality are evaluated, and the ratio at each SNR is calculated based on the direction of the inequality.

The ratio at the given SNR is denoted R(SNR).

6. The average performance curve is obtained by plotting R(SNR) versus SNR after repeating this procedure i times and averaging it accordingly. The value of i is taken to be one thousand in this thesis.

Consider a sinusoidal signal in presence of white noise, and let the desired frequency be given by π/N as stated in the problem. Assume that the performance curve has been obtained using the above method for white noise. The performance curve can be used to estimate the SNR at each ratio by reading the SNR from it.

In the above procedure, there is a fundamental problem we face in using the existing discrete-time Wirtinger inequalities. There is no guarantee that the signal generated in the above procedure satisfies the boundary conditions. Furthermore, it is not possible for the ratio to attain its maximum value of 1 if the phase γ takes on arbitrary values. Hence, the existing Wirtinger inequalities must be modified to forms that allow arbitrary phases with no boundary conditions attached to them. This is what we achieve in the next section.

3.2 Modification of Existing Inequalities

Consider inequality (1) in Section 2.3. To remove the boundary and phase conditions, we expand the circular convolution of the input and the impulse response. Comparing (2.42) and (2.43), we can write

$$\sum_{i=0}^{2N-1}(v[i+1]-v[i])^2 = 2\sum_{n=0}^{N-2}(x[n+1]-x[n])^2 + 2(x[0]+x[N-1])^2. \qquad (3.2)$$

Hence we can write that inequality as

$$\sum_{n=0}^{N-2}(x[n+1]-x[n])^2+(x[0]+x[N-1])^2 \geq 2\Big(1-\cos\frac{\pi}{N}\Big)\sum_{n=0}^{N-1}x[n]^2. \tag{3.3}$$

We do not need to attach any boundary conditions and (3.3) is true for any real signal. Now that we have removed the boundary condition, we have an equalizing signal that is more general. Recalling the proof of inequality (1), according to (2.54) the equalizing real signal is

$$\hat{x}[n]=A\cos\Big(\frac{\pi n}{N}+\gamma\Big), \qquad A,\gamma\in\mathbb{R}. \tag{3.4}$$

Since we do not have the boundary conditions on the signal, there is no need for $x[0]$ or $x[N-1]$ to be zero. Consequently, the arbitrary phase, γ, can have any value, and the inequality turns into equality when the signal is $\hat{x}[n]=A\cos\left(\frac{\pi n}{N}+\gamma\right)$. In other words, we can estimate the SNR of a sinusoid with frequency π/N with no restriction. Note that the embedded signal $\hat{v}[i]$ satisfies the condition $\hat{v}[i]=-\hat{v}[N+i]$, i.e.,

$$A\cos\Big(\frac{\pi(N+i)}{N}+\gamma\Big)=-A\cos\Big(\frac{\pi i}{N}+\gamma\Big) \tag{3.5}$$

Now we formally state the new result.

Inequality 3.2.1 *For any real signal $x[n]\in\mathbb{R}^N$, $n=0:N-1$, the following inequality holds*

$$\sum_{n=0}^{N-2}(x[n+1]-x[n])^2+(x[0]+x[N-1])^2 \geq 2\Big(1-\cos\frac{\pi}{N}\Big)\sum_{n=0}^{N-1}x[n]^2,$$

with equality if and only if $x[n]=\hat{x}[n]=A\cos\left(\pi n/N+\gamma\right)$, where $\gamma,A\in\mathbb{R}$.

Fig. 3.2 shows the average performance curve for inequality 3.2.1. We read the SNR from the performance curve, by the ratio obtained from the inequality for the observed signal. In other words, the SNR can be viewed as a function of the ratio R, where R is the ratio of the two sides of the inequality.

The performance curve has a transition region when it moves between the minimum ratio and the maximum ratio of 1. In this interval the function R is approximately linear and its derivative is almost constant. Therefore, we can easily estimate the SNR from the ratio of the inequality for the observed signal. At very high SNRs,

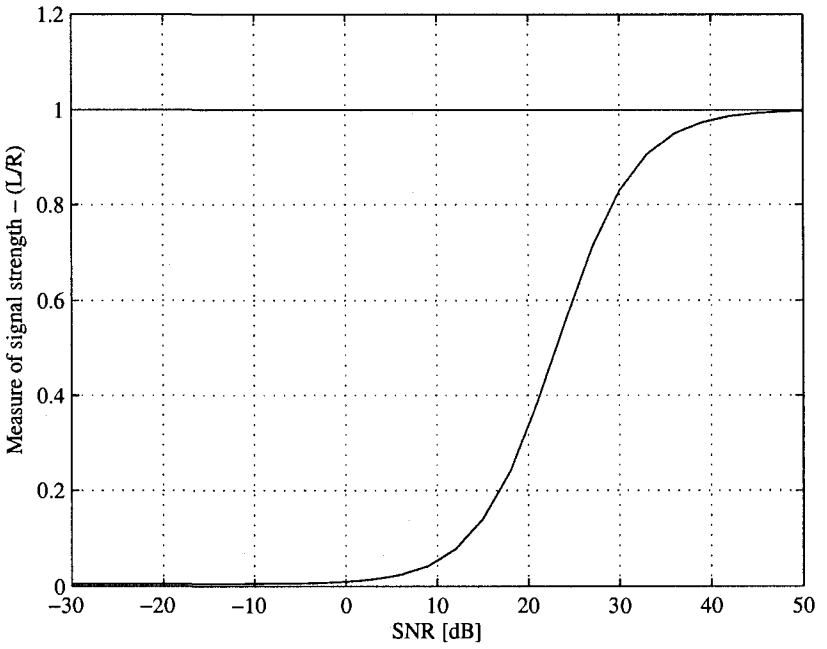

Figure 3.2: Average performance curve for inequality 3.2.1 with $N = 32$.

as can be seen from the figure, the ratio remains in a small interval close to one, and the increase in SNR does not change the ratio significantly. In other words, the performance curve saturates at high SNRs. This is not problematic since a very high

SNR signifies a strong signal. However, at low SNRs, where the signal is weak, the saturation of the performance curve results in a degradation of the ability to estimate the SNR from a calculated value of ratio for the observed signal. In the Fig. 3.2, the interval that can be viewed as a non-saturated region lies between the SNR values 0 dB and 40 dB. The ratio at low SNRs is approximately zero for the negative SNR values.

Inequality (1) was used to prove inequality (2) in Section 2.3. Here we use inequality 3.2.1 to find the modified version of inequality (2) instead. Note that the signal $x[n]$ is embedded in $q[i]$ as

$$q[i]\Big|_{i=0:2N-1} = (x[0], x[1], \cdots, x[N-1], x[N-1], \cdots, x[1], x[0]). \tag{3.6}$$

Hence, we can apply the inequality 3.2.1 and we have

$$\sum_{i=0}^{(2N-1)-1} (q[i+1]-q[i])^2 + (q[0]+q[2N-1])^2 \geq 2\Big(1-\cos\frac{\pi}{2N-1}\Big)\sum_{i=0}^{2N-1} x[n]^2. \tag{3.7}$$

Recalling the proof of inequality (2), we can write

$$2\sum_{n=0}^{N-2}(x[n+1]-x[n])^2 + 4x[0]^2 \geq 2\Big(1-\cos\frac{\pi}{2N-1}\Big)\Big(2\sum_{n=0}^{N-1} x[n]^2\Big). \tag{3.8}$$

After simplification we get

$$\sum_{n=0}^{N-2}(x[n+1]-x[n])^2 + 2x[0]^2 \geq 2\Big(1-\cos\frac{\pi}{2N-1}\Big)\sum_{n=0}^{N-1} x[n]^2. \tag{3.9}$$

The real equalizing signal is of the form $\hat{q}[i] = A\cos\left(\pi i/(2N-1)+\gamma\right)$ and according to the embedding method we should have

$$q[i] = q[2N-1-i]. \tag{3.10}$$

Therefore,

$$A\cos\left(\frac{\pi i}{2N-1}+\gamma\right)=A\cos\left(\pi-\frac{\pi i}{2N-1}+\gamma\right). \tag{3.11}$$

Now we expand (3.11)

$$\begin{aligned}&\cos\left(\frac{\pi i}{2N-1}\right)\cos\gamma-\sin\left(\frac{\pi i}{2N-1}\right)\sin\gamma\\&=-\cos\left(\frac{\pi i}{2N-1}\right)\cos\gamma-\sin\left(\frac{\pi i}{2N-1}\right)\sin\gamma.\end{aligned} \tag{3.12}$$

The sine terms cancel each other, and in order to satisfy (3.12) we must have $\cos\gamma=0$, which forces γ to be an odd multiple of $\pi/2$. Hence, the real equalizing signal $\hat{q}[i]=A\cos\left(\pi i/(2N-1)+\gamma\right)$, corresponds to $\hat{x}[n]=A\cos\left(\pi n/(2N-1)+\gamma\right)$, where γ is an odd multiple of $\pi/2$. Note that we are not able to eliminate the phase constraint in this case. The new inequality is stated below.

Inequality 3.2.2 *For any real signal $x[n]\in\mathbb{R}^N$, $n=0:N-1$, and $x[0]=0$, the following inequality holds*

$$\sum_{n=0}^{N-2}(x[n+1]-x[n])^2+2x[0]^2\geq 2\Big(1-\cos\frac{\pi}{2N-1}\Big)\sum_{n=0}^{N-1}x[n]^2,$$

with equality if and only if $x[n]=\hat{x}[n]=A\cos\left(\pi n/(2N-1)+\gamma\right)$, where γ is an odd multiple of $\pi/2$.

The average performance curve for inequality 3.2.2 is depicted in Fig. 3.3. The non-saturated region lies between the SNR values 10 dB and 50 dB. The ratio at low SNRs is approximately zero for SNR values less than 10 dB. Overall, the performance curve has moved to the right compared with Fig. 3.2.

Now consider inequality (3) in Section 2.3. Again we embed the signal $x[n]$ in $v[i]$

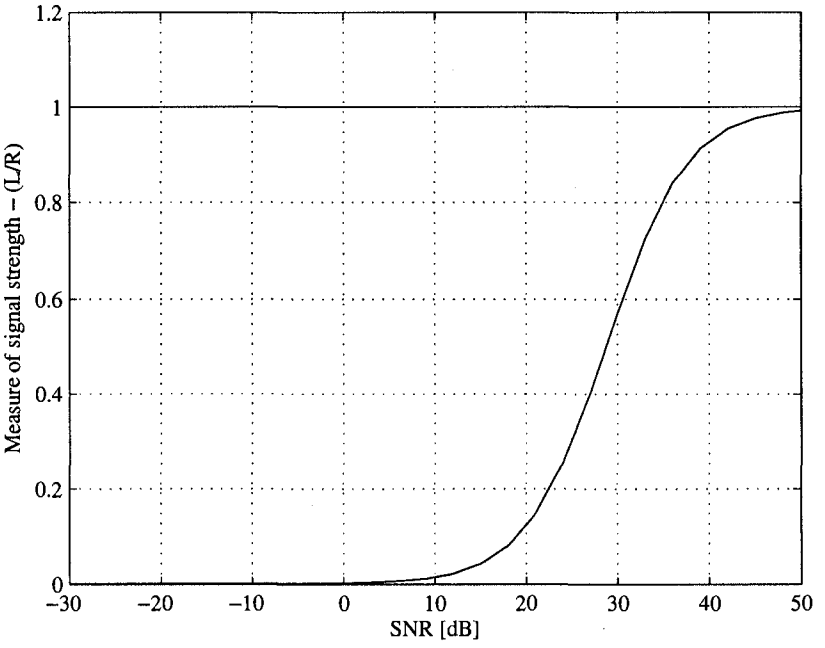

Figure 3.3: Average performance curve for inequality 3.2.2 with $N = 32$.

so that

$$\begin{aligned} v[i]\Big|_{i=0:2N-1} =& (x[0], x[1], \cdots, x[N-1], \\ & (-1)^{N-1}x[0], (-1)^{N-1}x[1], \cdots, (-1)^{N-1}x[N-1]). \end{aligned} \tag{3.13}$$

Therefore, the condition $\sum_{i=0}^{2N-1}(-1)^i v[i] = 0$ in part (b) of Proposition 1, is satisfied and we have

$$\sum_{i=0}^{2N-1}(v[i+1]-v[i])^2 \leq 2\Big(1+\cos\frac{2\pi}{2N}\Big)\sum_{i=0}^{2N-1} v[i]^2. \tag{3.14}$$

If we expand the left side we have

$$\begin{aligned} & \sum_{i=0}^{2N-1}(v[i+1]-v[i])^2 \\ & = 2\sum_{n=0}^{N-2}(x[n+1]-x[n])^2 + 2(x[0]-(-1)^{N-1}x[N-1])^2. \end{aligned} \tag{3.15}$$

On the other hand,

$$\sum_{i=0}^{2N-1} v[i]^2 = 2\sum_{n=0}^{N-1} x[n]^2. \tag{3.16}$$

Substitution of (3.16) and (3.15) in (3.14) gives

$$\sum_{n=0}^{N-2}(x[n+1]-x[n])^2 + (x[0]-(-1)^{N-1}x[N-1])^2 \leq 2\Big(1+\cos\frac{\pi}{N}\Big)\sum_{n=0}^{N-1} x[n]^2. \tag{3.17}$$

Recalling the proof of inequality (3) in Section 2.3, the equalizing real signal is $v[i] = A(-1)^i \cos\big(\pi i/N + \gamma\big)$. We do not have a boundary condition here but the condition $v[i] = (-1)^{N-1}v[N+i]$ should be verified.

$$(-1)^{N-1}v[N+i] = A(-1)^i \cos\big(\frac{\pi i}{N} + \gamma\big) = v[i]. \tag{3.18}$$

Consequently, γ can have any arbitrary value and the equalizing signal can be obtained by embedding the real signal $\hat{x}[n] = A(-1)^n \cos\big(\pi n/N + \gamma\big)$.

Inequality 3.2.3 *For any real signal $x[n] \in \mathbb{R}^N$, $n = 0 : N-1$, the following inequality holds*

$$\sum_{n=0}^{N-2}(x[n+1]-x[n])^2 + (x[0]-(-1)^{N-1}x[N-1])^2 \leq 2\Big(1+\cos\frac{\pi}{N}\Big)\sum_{n=0}^{N-1} x[n]^2,$$

with equality if and only if $x[n] = \hat{x}[n] = A(-1)^n \cos\big(\pi n/N + \gamma\big)$, where $\gamma, A \in \mathbb{R}$.

Fig. 3.4 shows the average performance curve for inequality 3.2.3. The non-saturated region lies between the SNR values 10 dB and 20 dB, which is lower than those for Fig. 3.2 and Fig. 3.3. The ratio at low SNRs is not zero in this case. However, the level of the curve in low SNRs is higher than the one in 3.2.1 and 3.2.2.

In inequality (4), we embed the the real signal $x[n]$, $n = 0 : N-1$ in $v[i]$ as

$$\begin{aligned} v[i]\Big|_{i=0:4N-2} &= (x[0], x[1], \cdots, x[N-1], x[N-1], x[N-2], \cdots, x[1], \\ &-x[0], -x[1], \cdots, -x[N-1], -x[N-1], -x[N-2], \cdots, -x[1]). \end{aligned} \tag{3.19}$$

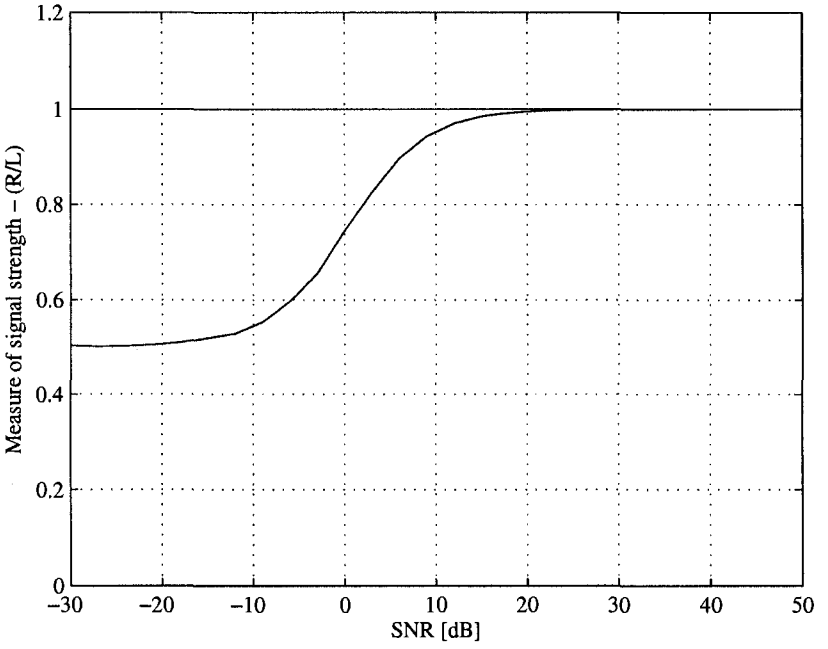

Figure 3.4: Average performance curve for inequality 3.2.3 with $N = 32$.

And as we explained in the proof of inequality (4) in Section 2.3, the conditions for applying part (c) of Proposition 1 are satisfied. Hence

$$\sum_{i=0}^{4N-3} (v[i+1] - v[i])^2 \leq 2\Big(1 + \cos\frac{4\pi}{4N-2}\Big) \sum_{i=0}^{4N-3} v[i]^2. \tag{3.20}$$

Now we expand the left side of inequality (3.20)

$$\begin{aligned} &\sum_{i=0}^{4N-3} (v[i+1] - v[i])^2 \\ &= 4\sum_{n=0}^{N-2} (x[n+1] - x[n])^2 - 2(x[1] - x[0])^2 + 2(x[1] + x[0])^2. \end{aligned} \tag{3.21}$$

It is also clear that

$$\sum_{i=0}^{4N-3} v[i]^2 = 4\sum_{n=0}^{N-1} x[n]^2 - 2x[0]^2. \tag{3.22}$$

If we substitute (3.21) and (3.22) in (3.20) we have

$$\begin{aligned} &2\sum_{n=0}^{N-1}(x[n+1]-x[n])^2-(x[1]-x[0])^2+(x[1]+x[0])^2 \\ &\leq 2\Big(1+\cos\frac{2\pi}{2N-1}\Big)\Big(2\sum_{n=0}^{N-1}x[n]^2-x[0]^2\Big). \end{aligned} \tag{3.23}$$

According to the proof of inequality (4), equalizing signal is of the form $\hat{v}[i] = A(-1)^i \cos\big(2\pi i/(2N-1)+\gamma\big)$. The embedded signal must satisfy $v[i] = v[2N-1-i]$, and we have

$$\hat{v}[2N-1-i] = -A(-1)^i \cos\big(\frac{-2\pi i}{2N-1}+\gamma\big). \tag{3.24}$$

Consequently, γ should be an odd multiple of $\pi/2$.

Inequality 3.2.4 *For any real signal $x[n] \in \mathbb{R}^N$, $n = 0 : N-1$, the following inequality holds*

$$\begin{aligned} &2\sum_{n=0}^{N-2}(x[n+1]-x[n])^2-(x[1]-x[0])^2+(x[1]+x[0])^2 \\ &\leq 2\Big(1+\cos\frac{2\pi}{2N-1}\Big)\Big(2\sum_{n=0}^{N-1}x[n]^2-x[0]^2\Big), \end{aligned}$$

with equality if and only if $x[n] = \hat{x}[n] = A(-1)^n \cos\big(2\pi n/(2N-1)+\gamma\big)$, where γ is an odd multiple of $\pi/2$.

Fig. 3.5 shows the average performance curve for inequality 3.2.4. The features of the performance curve are the same as the one for inequality 3.2.3.

Simulation results of the modified inequalities show a difference between the performance curves in Fig. 3.2 and Fig. 3.3, and the performance curves in Fig. 3.4 and Fig. 3.5. The difference is in level of the ratio at low SNRs which is higher in Fig. 3.4 and Fig. 3.5. This can be explained as follows. The impulse response of

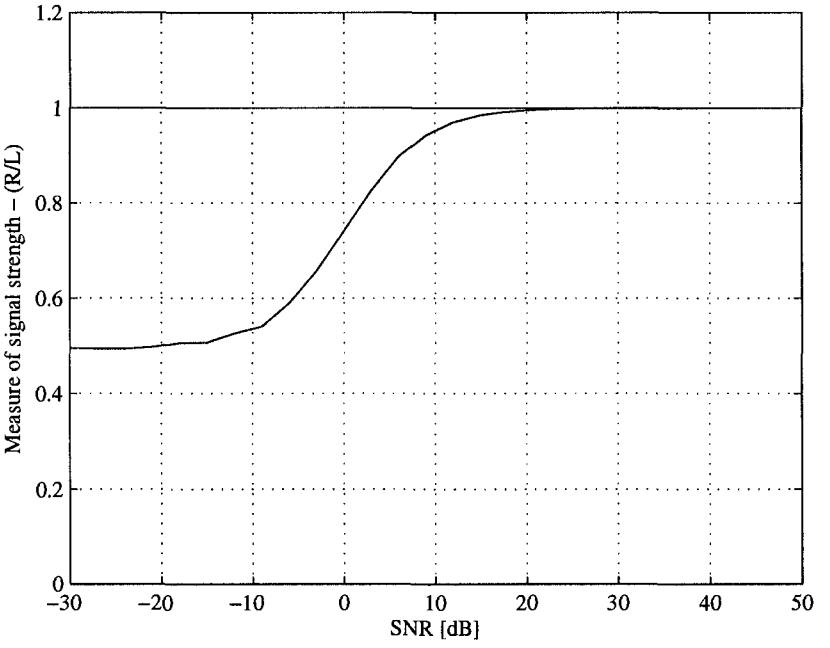

Figure 3.5: Average performance curve for inequality 3.2.4 with $N = 32$.

the forward difference system is that of a highpass filter (see Fig. 2.1). In inequality 3.2.1 and 3.2.2, we are looking for the minimum of the DFT of the impulse response. The equalizing signal is located at the frequency where the minimum modulus of the DFT of the impulse response occurs. We can interpret he left side of the inequalities, which is the energy of the output signal, as the area under the curve generated by the product of the DFT of the signal and the DFT of the impulse response. On the other hand, the right side of the inequalities can be viewed as the area under the curve obtained by the product of minimum modulus of the DFT of the impulse response and the DFT of the signal. Therefore, at low SNRs where the power of noise is much greater than the power of the signal, the area of the left side product is much greater than that of the right side product. Hence, the ratio becomes very small. Moreover,

inequalities 3.2.3 and 3.2.4 are based on the maximum modulus of the DFT of the impulse response. Thus, at low SNRs, there is a small difference between the area of the left side product and the area of the right side product, and the ratio becomes relatively high. This explains the high ratios at low SNRs when we use inequalities (4.1.3) and (4.1.4).

In 3.2.1 and 3.2.3, the restrictions on the boundary conditions and phase are completely removed. Comparing the simulation results, it can be seen that the performance curves are different for equalizing signals with different frequencies depending on the inequality that is used. Each performance curve gives an estimate of the SNR for the corresponding equalizing sinusoid with a known frequency.

As we mentioned, the best ability in estimating the SNR via the performance curve is achieved in the non-saturated region of the performance curve. Therefore, we are interested in making the non-saturated region in the performance curves as wide as possible. In order to see how the features of the performance curves change, we generalize the inequalities to the forms with different weights possessing different equalizing sinusoids.

Chapter 4

Generalizations of Discrete Wirtinger-Type Inequalities

In the previous chapter, we modified the existing inequalities to forms without boundary conditions and non-fixed phase. However, only a simple difference operation was considered as the impulse response of the circular convolution filter. In this chapter, our objective is to generalize the inequalities by considering weighted impulse responses. Furthermore, the impulse responses with wider gaps are considered and the corresponding inequalities are derived.

4.1 Generalization to Weighted Inequalities with Two Parameters

Let a and $b \in \mathbb{R}^+$ be positive numbers. We define the weighted forward difference system by the input-output relationship

$$y_{wf}[n] = ax[n+1] - bx[n], \tag{4.1}$$

and the impulse response

$$h_{wf}[n] = \begin{cases} -b, & n = 0 \\ a, & n = N-1 \\ 0, & \text{otherwise.} \end{cases}, \quad 0 \le n \le N-1 \tag{4.2}$$

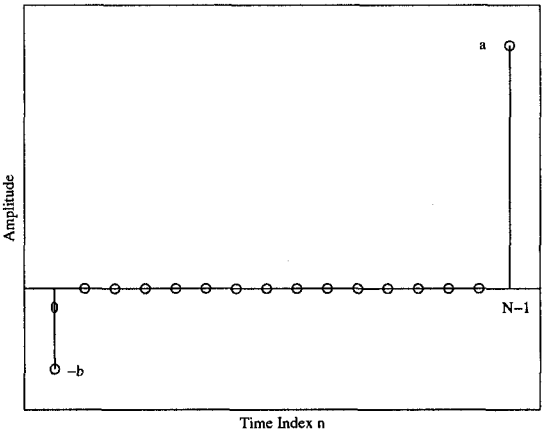

Figure 4.1: $h_{wf}[n]$ - impulse response of the weighted forward difference system.

Fig. 4.1 illustrates the impulse response $h_{wf}[n]$. The DFT of $h_{wf}[n]$ is

$$H_{wf}[k] = ae^{j(2\pi/N)k} - b, \quad 0 \le k \le N-1, \tag{4.3}$$

and the squared norm of $H_{wf}[k]$ is

$$|ae^{j(2\pi/N)k} - b|^2 = a^2 + b^2 - 2ab\cos\frac{2\pi k}{N}, \quad 0 \le k \le N-1. \tag{4.4}$$

Now consider the embedded signal

$$v[i]\Big|_{i=0:2N-1} = (x[0], x[1], \cdots, x[N-1], -x[0], -x[1], \cdots, -x[N-1]). \tag{4.5}$$

Recalling part (a) of Proposition 1, the minimum of $(a^2 + b^2 - 2ab\cos\frac{2\pi k}{N})$ is attained at $k = 1$ and $k = N-1$, and is equal to $(a^2 + b^2 - 2ab\cos\frac{2\pi}{N})$. Thus, we can write

$$\sum_{i=0}^{2N-1}(av[i+1] - bv[i])^2 \ge \left(a^2 + b^2 - 2ab\cos\frac{\pi}{N}\right)\sum_{i=0}^{2N-1} v[i]^2. \tag{4.6}$$

Expanding the left side of (4.6), we have

$$\sum_{i=0}^{2N-1}(av[i+1] - bv[i])^2 = 2\sum_{n=0}^{N-2}(ax[n+1] - bx[n])^2 + 2(ax[0] + bx[N-1])^2. \tag{4.7}$$

Thus the following inequality is obtained as a generalized form of inequality 3.2.1,

Inequality 4.1.1 *For any real signal $x[n] \in \mathbb{R}^N$, $n = 0 : N-1$, the following inequality holds*

$$\sum_{n=0}^{N-2}(ax[n+1] - bx[n])^2 + (ax[0] + bx[N-1])^2 \ge \left(a^2 + b^2 - 2ab\cos\frac{\pi}{N}\right)\sum_{n=0}^{N-1} x[n]^2$$

where $ab > 0$. Equality holds if and only if $x[n] = \hat{x}[n] = A\cos(\pi n/N + \gamma)$, where $\gamma, A \in \mathbb{R}$.

Some average performance curve for inequality 4.1.1 are depicted in Fig. 4.2. It can be seen that by changing the weights we can get wider transition regions, and consequently, wider non-saturated region. Moreover, one should note that the level

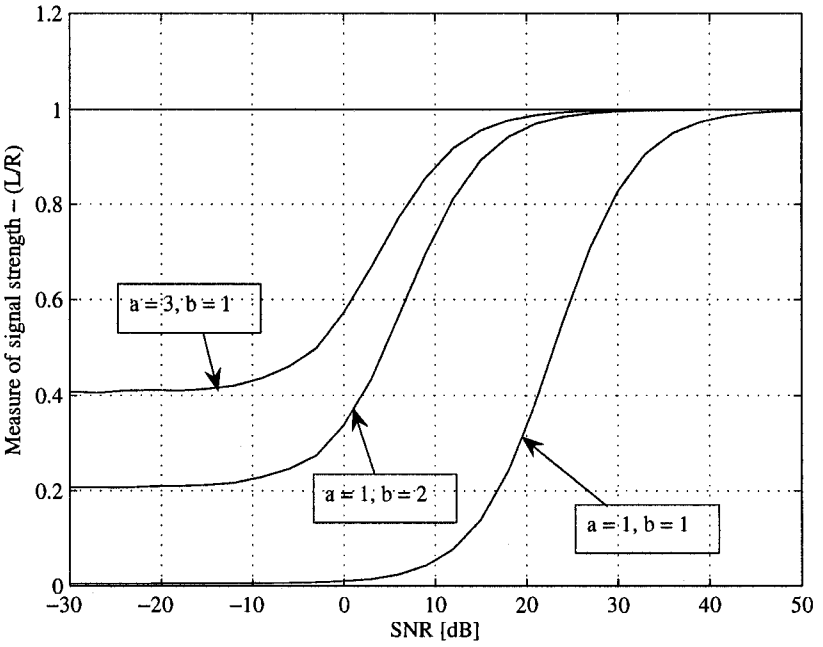

Figure 4.2: Average performance curves for inequality 4.1.1 with (1) $a = b = 1$, (2) $a = 1$ and $b = 2$, (3) $a = 3$, $b = 1$, and $N = 32$.

at low SNRs in graph (3) changes while the level in graph (1) is close to zero for a wide range of SNR's.

The other inequalities can be found using the same approach. The results are given below.

Inequality 4.1.2 *For any real signal* $x[n] \in \mathbb{R}^N$, $n = 0 : N-1$, *the following inequality holds*

$$\sum_{n=0}^{N-2}(ax[n+1]-bx[n])^2+\sum_{n=0}^{N-2}(bx[n+1]-ax[n])^2+((a+b)x[0])^2+((a-b)x[N-1])^2$$
$$\geq 2\Big(a^2+b^2-2ab\cos\frac{\pi}{2N-1}\Big)\sum_{n=0}^{N-1}x[n]^2,$$

where $ab > 0$. *Equality holds if and only if* $x[n] = \hat{x}[n] = A\cos\big(\pi n/(2N-1)+\gamma\big)$,

where γ is an odd multiple of $\pi/2$ and $A \in \mathbb{R}$.

Fig. 4.3 shows some average performance curves for inequality 4.1.2. The changes are similar to those in Fig. 4.2.

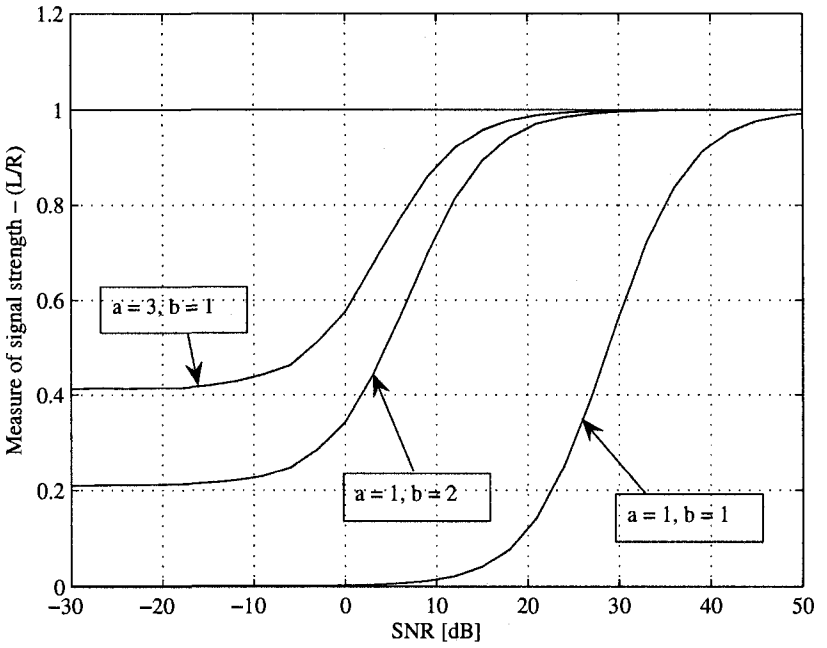

Figure 4.3: Average performance curves for inequality 4.1.2 with (1) $a = b = 1$, (2) $a = 1$ and $b = 2$, (3) $a = 3$, $b = 1$, and $N = 32$, $\gamma = -\pi/2$.

Inequality 4.1.3 *For any real signal $x[n] \in \mathbb{R}^N$, $n = 0 : N-1$, the following inequality holds*

$$\sum_{n=0}^{N-2}(ax[n+1]-bx[n])^2+(ax[0]-b(-1)^{N-1}x[N-1])^2 \leq \left(a^2+b^2+2ab\cos\frac{\pi}{N}\right)\sum_{n=0}^{N-1}x[n]^2,$$

where $ab > 0$. Equality holds if and only if $x[n] = \hat{x}[n] = A(-1)^n \cos\left(\pi n/N + \gamma\right)$, where $\gamma, A \in \mathbb{R}$.

Fig. 4.4 shows some average performance curves for inequality 4.1.3. It is clear that the performance curves in Fig. 4.4 do not change significantly by changing the values of the weights despite Fig. 4.2 and Fig. 4.3.

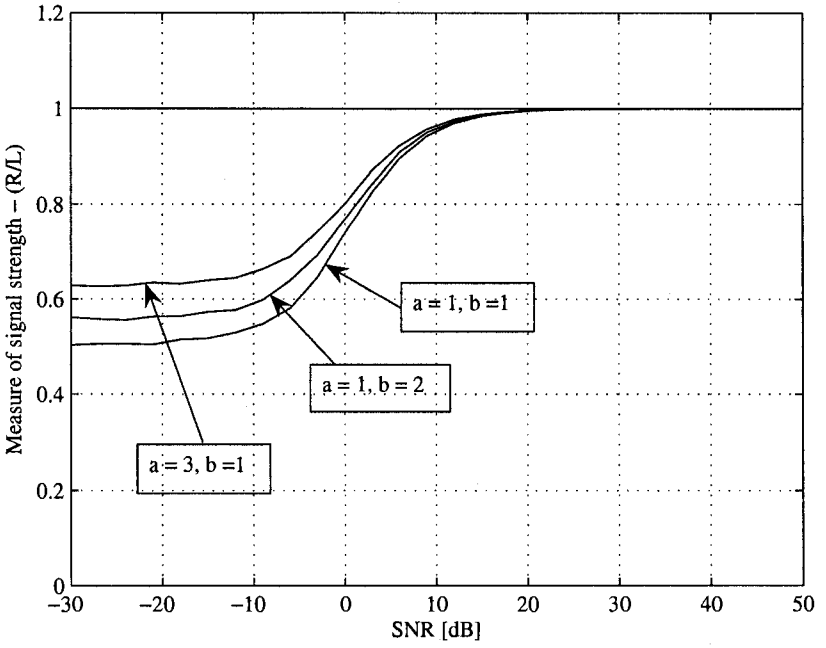

Figure 4.4: Average performance curves for inequality 4.1.3 with ((1) $a = b = 1$, (2) $a = 1$ and $b = 2$, (3) $a = 3$, $b = 1$, and $N = 32$.

Inequality 4.1.4 *For any real signal* $x[n] \in \mathbb{R}^N$, $n = 0 : N-1$, *the following inequality holds*

$$\sum_{n=0}^{N-2}(ax[n+1]-bx[n])^2+\sum_{n=0}^{N-2}(bx[n+1]-ax[n])^2$$

$$+((a-b)x[N-1])^2+4abx[0]x[1]$$

$$\leq \left(a^2+b^2+2ab\cos\frac{2\pi}{2N-1}\right)\left(2\sum_{n=0}^{N-1}x[n]^2-x[0]^2\right)$$

where $ab > 0$. *Equality holds if and only if* $x[n] = \hat{x}[n] = A(-1)^n \cos\big(2\pi n/(2N-1)+\gamma\big)$, *where* γ *is an odd multiple of* $\pi/2$.

Some average performance curves for inequality 4.1.4 is shown in Fig. 4.5. The changes in the performance curves are the same as Fig. 4.4.

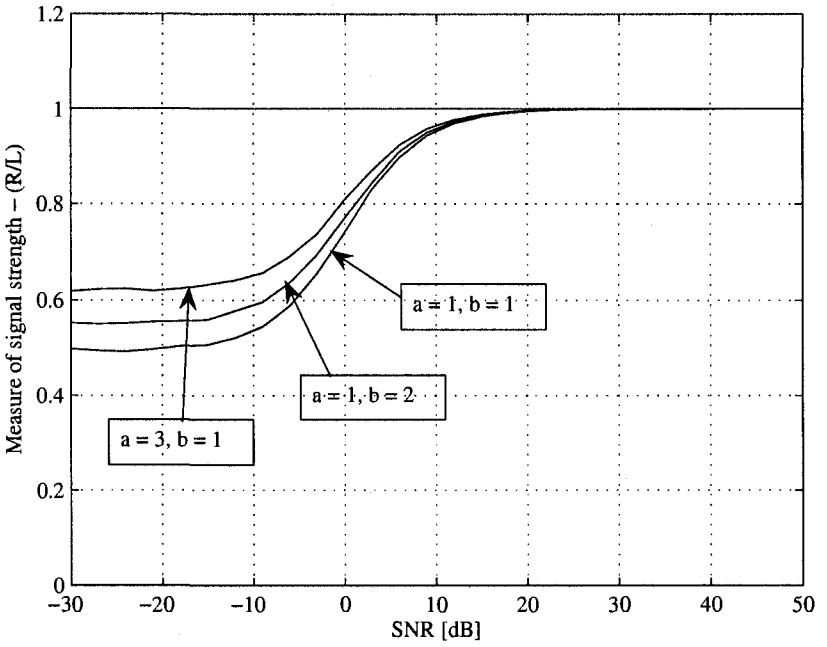

Figure 4.5: Average performance curves for inequality 4.1.4 with (1) $a = b = 1$, (2) $a = 1$ and $b = 2$, (3) $a = 3$, $b = 1$, and $N = 32$, $\gamma = -\pi/2$.

One should note that if $h_{wf}[0]$ and $h_{wf}[N-1]$ have the same signs, or $ab < 0$, the squared moduli of the DFT coefficients impulse response becomes

$$|ae^{j(2\pi/N)k} + b|^2 = a^2 + b^2 + 2ab\cos\frac{2\pi k}{N}, \quad 0 \le k \le N-1. \tag{4.8}$$

The maximum of $(a^2 + b^2 + 2ab\cos\frac{2\pi k}{N})$ occurs at the point where the minimum of $(a^2 + b^2 - 2ab\cos\frac{2\pi k}{N})$ is located. On the other hand, at the maximum point of

$(a^2 + b^2 - 2ab\cos\frac{2\pi k}{N})$, the minimum of $(a^2 + b^2 + 2ab\cos\frac{2\pi k}{N})$ occurs. Hence, the direction of the inequality has to be changed when a and b have opposite signs. This is important in using the inequalities with negative values of a and b.

Based on our observations, the only factor that affects the performance of the inequalities is the impulse response of the system. Therefore, by changing the structure of the impulse response, we may be able to find better inequalities. In the next section, we study the changes that can be made to the structure of the impulse response.

4.2 Other New Two-Parameter Inequalities

4.2.1 Two Weights with a Gap of One

Thinking circularly, the weights of the impulse response used in 4.1 are adjacent. In other words, there is no circular gap between the two non-zero weights. As the first attempt to changing the structure of the impulse response, we increase the gap between the two non-zero weights by one.

Consider the impulse response in Fig. 4.6. The DFT of this impulse response is

$$H_{g1}[k] = ae^{j(4\pi/N)k} - b, \quad 0 \leq k \leq N-1, \tag{4.9}$$

and the squared norm becomes

$$|ae^{j(4\pi/N)k} - b|^2 = a^2 + b^2 - 2ab\cos\frac{4\pi k}{N}, \quad 0 \leq k \leq N-1. \tag{4.10}$$

To find the maximum and minimum of $a^2 + b^2 - 2ab\cos(4\pi k/N)$, the first derivative

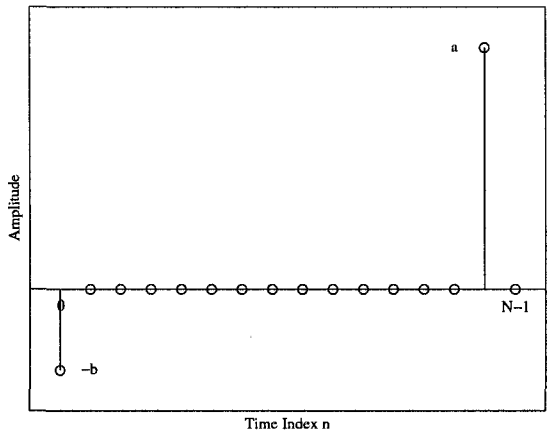

Figure 4.6: $h_{g1}[n]$ - impulse response of the system with a circular gap of one between the two non-zero weights.

is set to zero

$$\frac{d}{dk}(a^2 + b^2 - 2ab\cos(4\pi k/N)) = (8ab\pi/N)\sin(4\pi k/N) = 0. \tag{4.11}$$

This implies that the maximum or minimum happen when $k = mN/4$, $m = 0, 1, 2, 3$. The sign of the second derivative

$$\frac{d^2}{dk^2}(a^2 + b^2 - 2ab\cos(4\pi k/N)) = (32ab\pi^2/N^2)\cos(4\pi k/N) \tag{4.12}$$

determines whether the critical point is a maximum or a minimum. Since a and b are positive numbers, the sign of $\cos(4\pi k/N)$ governs the sign of the second derivative. The discrete-valued indices, k_i, is the location of i-th extremum point for $i = 1, 2, 3, 4$, and is a multiple of $N/4$ in this case. Therefore, for k_i to be an integer, four cases are considered.

1. $N \overset{4}{\equiv} 0$ $(N = 4l)$.

As an example, Fig. 4.7 shows the amplitude of $a^2 + b^2 - 2ab\cos(4\pi k/N)$ for $N = 16$.

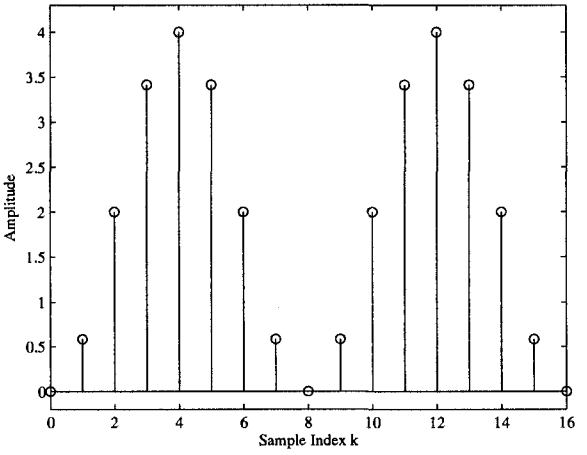

Figure 4.7: $a^2 + b^2 - 2ab\cos(4\pi k/N)$ for $a = b = 1$, and $N = 16$.

At $m = 0$ we have $k_1 = 0$, and we have a minimum. At $m = 1$, k_2 is $N/4$. Since N is a multiple of 4, k_{m2} is an integer, and we have a maximum. There is also a minimum at $k_3 = N/2$ and a maximum at $k_4 = 3N/4$. This can be verified for $N = 16$ in Fig. 4.7. Since the minimum is zero for $N = 4l$, the inequality will be $\sum_n (ax[n+2] - bx[n])^2 \geq 0$ which is trivial. Consequently, we should consider the next smallest value and embed the signal in such a way that zero magnitudes are avoided. The zero magnitudes located at $k_1 = 0$ and $k_3 = N/2$ and the conditions $\sum_{n=0}^{N} x[n] = 0$ and $\sum_{n=0}^{N} (-1)^n x[n] = 0$ should be satisfied at the same time which is not possible due to the embedding methods that we have to satisfy. Hence, we focus on the maximum points k_2 and k_4.

The maximum value of $|H_{g1}[k]|$ is

$$a^2 + b^2 - 2ab\cos\frac{4\pi N}{4N} = (a+b)^2, \tag{4.13}$$

and the inequality becomes

$$\sum_{n=0}^{N-1}(ax[n+2] - bx[n])^2 \leq (a+b)^2 \sum_{n=0}^{N-1} x[n]^2, \tag{4.14}$$

and the equalizing signal is of the form $\alpha e^{j(2\pi/N)(N/4)n} + \beta e^{j(2\pi/N)(3N/4)n}$. Applying the condition $\alpha = \beta^*$ to ensure that the equalizing signal is real, we have

$$\begin{aligned} &|\alpha|e^{j((2\pi/N)(N/4)n+\theta_\alpha)} + |\alpha|e^{j((2\pi/N)(3N/4)n-\theta_\alpha)} = \\ &2\alpha\cos(\pi n/2 + \theta_\alpha). \end{aligned} \tag{4.15}$$

Hence the equalizing real signal is $x[n] = \hat{x[n]} = A\cos(\pi n/2 + \gamma)$.

Inequality 4.2.1 *For any real signal $x[n] \in \mathbb{R}^N$, $n = 0 : N-1$, and $N = 4l$ where $l \in \mathbb{R}$, the following inequality holds*

$$\sum_{n=0}^{N-1}(ax[n+2] - bx[n])^2 \leq (a+b)^2 \sum_{n=0}^{N-1} x[n]^2$$

with equality if and only if $x[n] = \hat{x}[n] = A\cos(\pi n/2 + \gamma)$, where A, $\gamma \in \mathbb{R}$.

Some average performance curves are depicted in Fig. 4.8. comparing performance curves of Fig. 4.8 to those one in Fig. 4.4, we realize that they are very similar. they have a wide non-saturated region. At low SNRs still the level of the performance curves is flat. It can be also seen that the performance curves do not change significantly by changing the values of the weights.

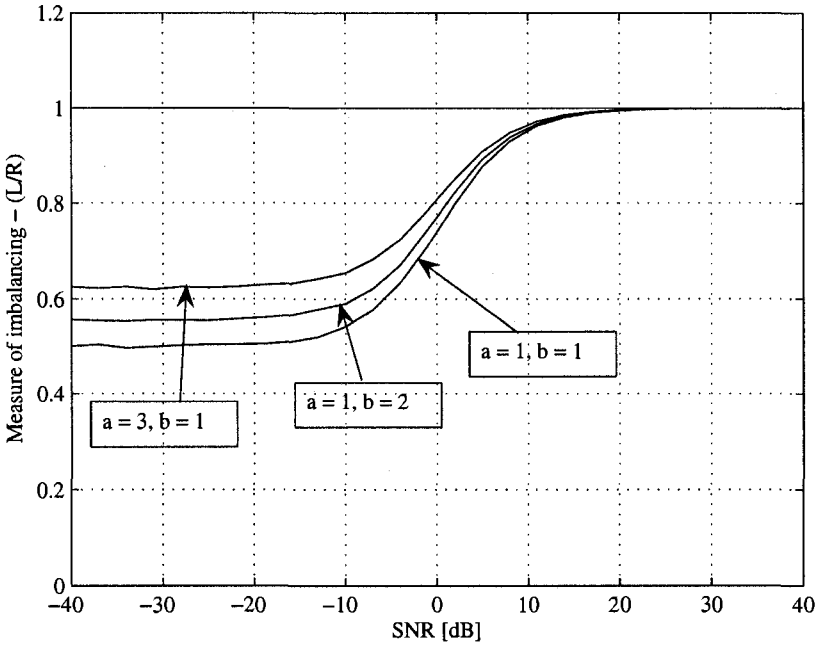

Figure 4.8: Average performance curves for inequality 4.2.1 with (1) $a = b = 1$, (2) $a = 1$ and $b = 2$, (3) $a = 3$, $b = 1$, and $N = 32$.

2. $N \overset{4}{\equiv} 1$ $(N = 4l + 1)$.

Fig. 4.9 shows the amplitude of $a^2 + b^2 - 2ab\cos(4\pi k/N)$ for $N = 17$.

- For $m = 0$ there is a minimum which is zero.
- For $m = 1$, k_2 is $N/4$ or, equivalently, $k_2 = (4l + 1)/4$. Since this value is not an integer, $k_2$will be replaced by the nearest adjacent integer value. Therefore, this value has to be rounded to its nearest integer, and we have $k_2 = l$, or equivalently, $k_2 = (N - 1)/4$.
- For $m = 2$, there is a minimum at $k_3 = 2l+1/2$. This value can be rounded to both $2l + 1$ or $2l$, which give $k_3 = (2N + 2)/4$ or $k_3 = (2N - 2)/4$,

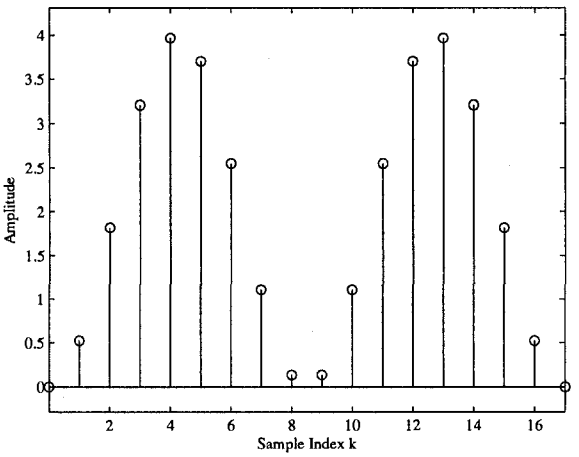

Figure 4.9: $a^2 + b^2 - 2ab\cos(4\pi k/N)$ for $a = b = 1$, and $N = 17$.

respectively.

- For $m = 3$, we have a maximum at $k_4 = 3N/4 = 3(4l + 1)/4$, which can be rounded to $3l + 1$ or, equivalently, to $k_4 = (3N + 1)/4$.

As we can see in Fig. 4.9, the two maximum points have the same magnitude which is $a^2 + b^2 + 2ab\cos\frac{\pi}{N}$. Consequently, we have

$$\sum_{n=0}^{N-1}(ax[n+2] - bx[n])^2 \leq \left(a^2 + b^2 + 2ab\cos(\pi/N)\right)\sum_{n=0}^{N-1}x[n]^2, \tag{4.16}$$

and the equalizing signal is of the form $\alpha e^{j(2\pi/N)((N-1)/4)n} + \beta e^{j(2\pi/N)((3N+1)/4)n}$. Now we find the real signal by applying the condition $\alpha = \beta^*$ to ensure that the equalizing signal is real.

$$\begin{aligned} &|\alpha|e^{j((2\pi/N)((N-1)/4)n+\theta_\alpha)} + |\alpha|e^{j((2\pi/N)((3N+1)/4)n-\theta_\alpha)} = \\ &2\alpha\cos(\pi n/2 - \pi n/2N + \theta_\alpha). \end{aligned} \tag{4.17}$$

Hence the equalizing real signal is $x[n] = \hat{x}[n] = A\cos(\pi n/2 - \pi n/2N + \gamma)$. The above results are summarized below.

Inequality 4.2.2 *For any real signal* $x[n] \in \mathbb{R}^N$, $n = 0 : N-1$, $N = 4l+1$ *and* $l \in \mathbb{R}$, *the following inequality holds*

$$\sum_{n=0}^{N-1}(ax[n+2] - bx[n])^2 \leq \left(a^2 + b^2 + 2ab\cos(\pi/N)\right)\sum_{n=0}^{N-1} x[n]^2$$

with equality if and only if $x[n] = \hat{x}[n] = A\cos(\pi n/2 - \pi n/2N + \gamma)$, *where* A, $\gamma \in \mathbb{R}$.

Fig. 4.10 shows the simulation results for inequality 4.2.2. Here the performance curves are almost the same as those in Fig. 4.8.

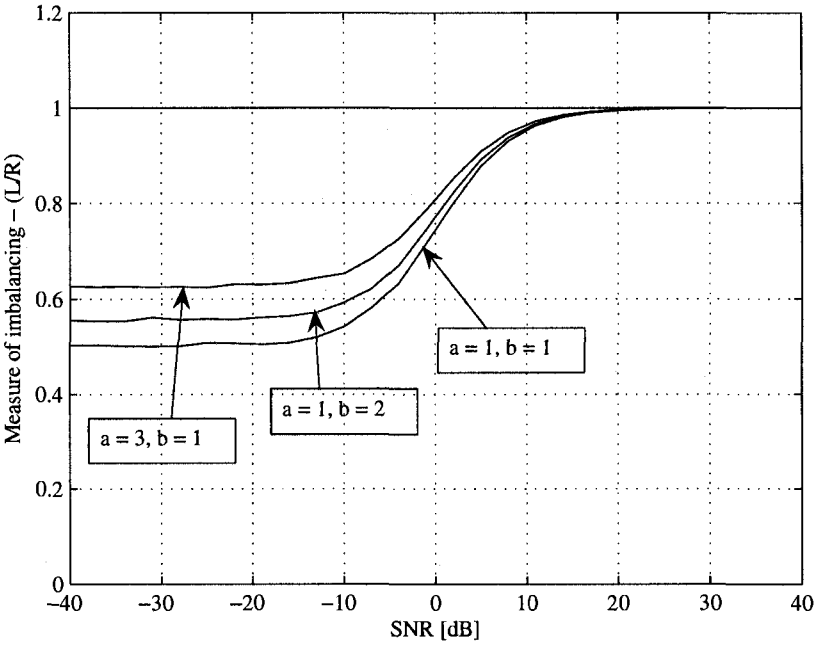

Figure 4.10: Average performance curves for inequality 4.2.2 with (1) $a = b = 1$, (2) $a = 1$ and $b = 2$, (3) $a = 3$, $b = 1$, and $N = 33$.

For the minimum points $k_3 = (2N \pm 2)/4$ we have to satisfy the condition $\sum_{n=0}^{N} x[n] = X[0] = 0$, to avoid the other minimum point at $k = 0$. The

minimum magnitude at $k_3 = (2N \pm 2)/4$ is

$$a^2 + b^2 - 2ab\cos\frac{4\pi(2N-2)}{4N} = a^2 + b^2 - 2ab\cos\frac{2\pi}{N}, \tag{4.18}$$

and the inequality becomes

$$\sum_{n=0}^{N-1}(ax[n+2] - bx[n])^2 \geq \Big(a^2 + b^2 - 2ab\cos(2\pi/N))\Big)\sum_{n=0}^{N-1}x[n]^2, \tag{4.19}$$

with equality if and only if $x[n] = \hat{x}[n] = \alpha e^{j(2\pi/N)((2N-2)/4)n} + \beta e^{j(2\pi/N)((2N+2)/4)n}$.

Now we apply $\alpha = \beta^*$ to ensure that the equalizing signal is real, and we have

$$\begin{aligned} &|\alpha|e^{j((2\pi/N)((2N-2)/4)n+\theta_\alpha)} + |\alpha|e^{j((2\pi/N)((2N+2)/4)n-\theta_\alpha)} = \\ &2\alpha(-1)^n\cos(\pi n/N + \theta_\alpha). \end{aligned} \tag{4.20}$$

Therefore, the equalizing real signal is $x[n] = \hat{x}[n] = A(-1)^n\cos(\pi n/N + \gamma)$ where A, $\gamma \in \mathbb{R}$. To relax the bounding condition, we embed the signal $x[n]$ as

$$v[i]\Big|_{i=0:2N-1} = (x[0], x[1], \cdots, x[N-1], -x[0], -x[1], \cdots, -x[N-1]), \tag{4.21}$$

and we have

$$\sum_{i=0}^{2N-1}(av[i+2] - bv[i])^2 \geq \Big(a^2 + b^2 - 2ab\cos(\pi/N)\Big)\sum_{i=0}^{2N-1}v[i]^2. \tag{4.22}$$

On the other hand, if we expand the left side of (4.22), we have

$$\begin{aligned} \sum_{i=0}^{2N-1}(av[i+2] - bv[i])^2 &= 2\sum_{n=0}^{N-2}(ax[n+2] - bx[n])^2 \\ &+ 2(ax[0] + bx[N-2])^2 + 2(ax[1] + bx[N-1])^2. \end{aligned} \tag{4.23}$$

Hence, the new inequality is

$$\begin{aligned} &\sum_{n=0}^{N-2}(ax[n+2] - bx[n])^2 + (ax[0] + bx[N-2])^2 + (ax[1] + bx[N-1])^2 \\ &\geq \big(a^2 + b^2 - 2ab\cos(\pi/N)\big)\sum_{n=0}^{N-1}x[n]^2, \end{aligned} \tag{4.24}$$

and the equalizing signal is $x[n] = \hat{x}[n] = A(-1)^n \cos(\pi n/N + \gamma)$. But the condition $v[i] = -v[i+N]$ is never satisfied because the signal is not completely symmetric, i.e.,

$$\begin{aligned} -v[i+N] &= -A(-1)^{(i+N)} \cos(\pi/2 + \pi i/(2N) + \gamma) \\ &\neq A(-1)^i \cos(\pi i/(2N) + \gamma). \end{aligned} \tag{4.25}$$

This implies that we cannot use the embedding in 4.21 in this case and, consequently, we can not relax the boundary conditions. Hence, the inequality based on the minimum value of $a^2 + b^2 - 2ab\cos(4\pi k/N)$ when $N = 4l + 2$ cannot be derived.

3. $N \overset{4}{\equiv} 2$ $(N = 4l + 2)$.

Fig. 4.11 shows the amplitude of $a^2 + b^2 - 2ab\cos(4\pi k/N)$ for $N = 18$.

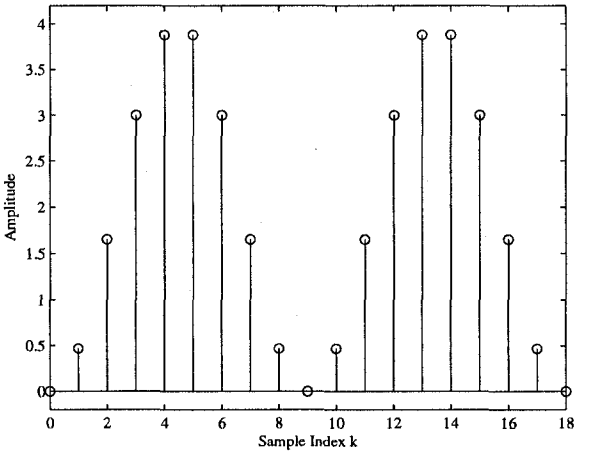

Figure 4.11: $a^2 + b^2 - 2ab\cos(4\pi k/N)$ for $a = b = 1$, and $N = 18$.

- The minimum is zero and is attained for $m = 0$ and $m = 2$ at $k_1 = 0$ and $k_3 = N/2$. Like case 1, the conditions $\sum_{n=0}^{N-1} x[n] = 0$ and $\sum_{n=0}^{N-1}(-1)^n x[n] =$

0 can not be satisfied at the same time, so we derive the inequalities for the maximum.

- At $m = 1$, we have $k_2 = (4l + 2)/4$. It can be rounded to $l + 1$ or, l, or, equivalently, to $(N + 2)/4$ or $(N - 2)/4$, respectively.
- For $m = 3$, we have another two maximum points $(3N + 2)/4$, and $(3N - 2)/4$.

The amplitude at these points is $a^2 + b^2 + 2ab\cos\frac{2\pi}{N}$, and the inequality is as follows

$$\sum_{n=0}^{N-1}(ax[n+2] - bx[n])^2 \leq \left(a^2 + b^2 + 2ab\cos(2\pi/N)\right)\sum_{n=0}^{N-1}x[n]^2. \tag{4.26}$$

The equalizing signal is of the form

$$\begin{aligned} x[n] = \hat{x}[n] = \alpha_1 e^{j(2\pi/N)((N-2)/4)n} + \alpha_2 e^{j(2\pi/N)((N+2)/4)n} \\ + \beta_2 e^{j(2\pi/N)((3N-2)/4)n} + \beta_1 e^{j(2\pi/N)((3N+2)/4)n}. \end{aligned} \tag{4.27}$$

The component pairs at $k_1 = (N-2)/4$ and $k_4 = (3N+2)/4$, and at $k_2 = (N+2)/4$ and $k_3 = (3N-2)/4$ are complex conjugate. Therefore by enforcing $\alpha_1 = \beta_1^*$ and $\alpha_2 = \beta_2^*$, $\hat{x}[n]$ becomes real and we have $x[n] = \hat{x}[n] = A_1\cos(\pi n/2 - \pi n/N + \gamma_1) + A_2\cos(\pi n/2 + \pi n/N + \gamma_2)$ where $A_1, A_2, \gamma_1, \gamma_2 \in \mathbb{R}$.

Inequality 4.2.3 *For any real signal $x[n] \in \mathbb{R}^N$, $n = 0 : N-1$, $N = 4l + 2$, and $l \in \mathbb{R}$, the following inequality holds*

$$\sum_{n=0}^{N-1}(ax[n+2] - bx[n])^2 \leq \left(a^2 + b^2 + 2ab\cos(2\pi/N)\right)\sum_{n=0}^{N-1}x[n]^2,$$

with equality if and only if $x[n] = \hat{x}[n] = A_1\cos(\pi n/2 - \pi n/N + \gamma_1) + A_2\cos(\pi n/2 + \pi n/N + \gamma_2)$, where $A_1, A_2, \gamma_1, \gamma_2 \in \mathbb{R}$.

Note that we have a new type of the equalizing signal which contains more than one frequency. The simulation results are provided in Fig. 4.12. The performance curves are almost the same as those in Fig. 4.8.

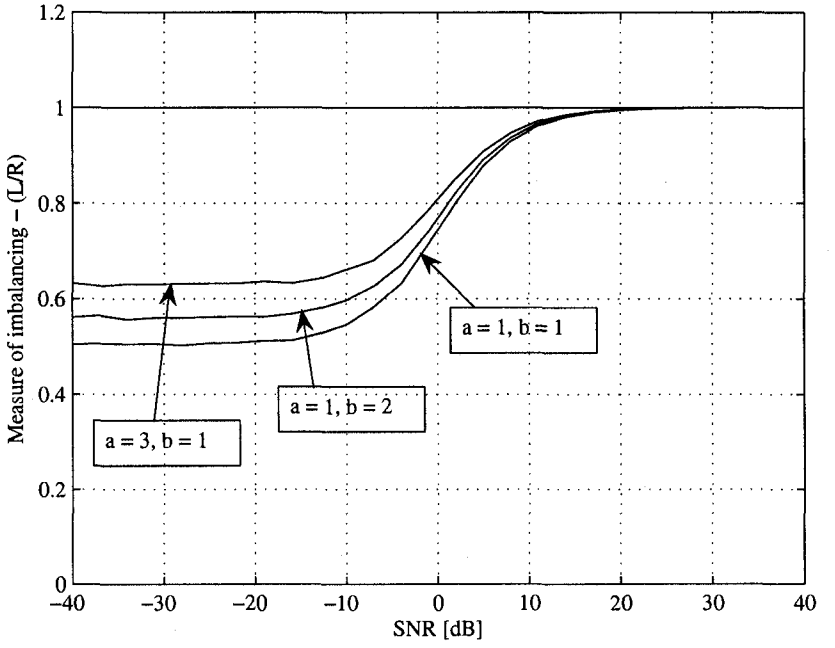

Figure 4.12: Average performance curves for inequality 4.2.3 with (1) $a = b = 1$, (2) $a = 1$ and $b = 2$, (3) $a = 3$, $b = 1$, and $N = 34$.

4. $N \overset{4}{\equiv} 3$ $(N = 4l + 3)$.

In this case,

- The minimum is zero as well and the next smallest value is attained at $k_3 = (2N \pm 1)/4$ like case 2. Therefore, we cannot achieve the embedding.
- For $m = 1$, the maximum point is $k_2 = (4l + 3)/4$. This value has to be rounded to its nearest integer, and we have $k_2 = l + 1$ or, equivalently,

$k_2 = (N+1)/4$.

- The other maximum point is located at $k_4 = (3N-1)/4$. This can be verified in Fig. 4.13.

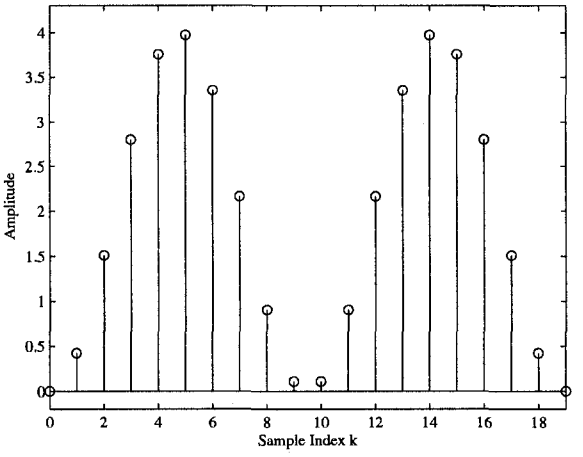

Figure 4.13: $a^2 + b^2 - 2ab\cos(4\pi k/N)$ for $a = b = 1$, and $N = 19$.

The maximum magnitude is $a^2 + b^2 + 2ab\cos\frac{\pi}{N}$. Therefore, the inequality is the same as (4.16), and the equalizing signal is

$$x[n] = \hat{x}[n] = \alpha e^{j(2\pi/N)((N+1)/4)n} + \beta e^{j(2\pi/N)((3N-1)/4)n}. \tag{4.28}$$

The real signal can be found in the same way as case 2, and it is $x[n] = \hat{x}[n] = A\cos(\pi n/2 + \pi n/2N + \gamma)$. The results is summarized below.

Inequality 4.2.4 *For any real signal $x[n] \in \mathbb{R}^N$, $n = 0 : N-1$, $N = 4l+3$, and $l \in \mathbb{R}$, the following inequality holds*

$$\sum_{n=0}^{N-1}(ax[n+2] - bx[n])^2 \leq \left(a^2 + b^2 + 2ab\cos(\pi/N)\right)\sum_{n=0}^{N-1} x[n]^2,$$

with equality if and only if $x[n] = \hat{x}[n] = A\cos(\pi n/2 + \pi n/2N + \gamma)$, *where* A, $\gamma \in \mathbb{R}$.

The performance curves are shown in Fig. 4.14. Here the performance curves are the same as the one in Fig. 4.8.

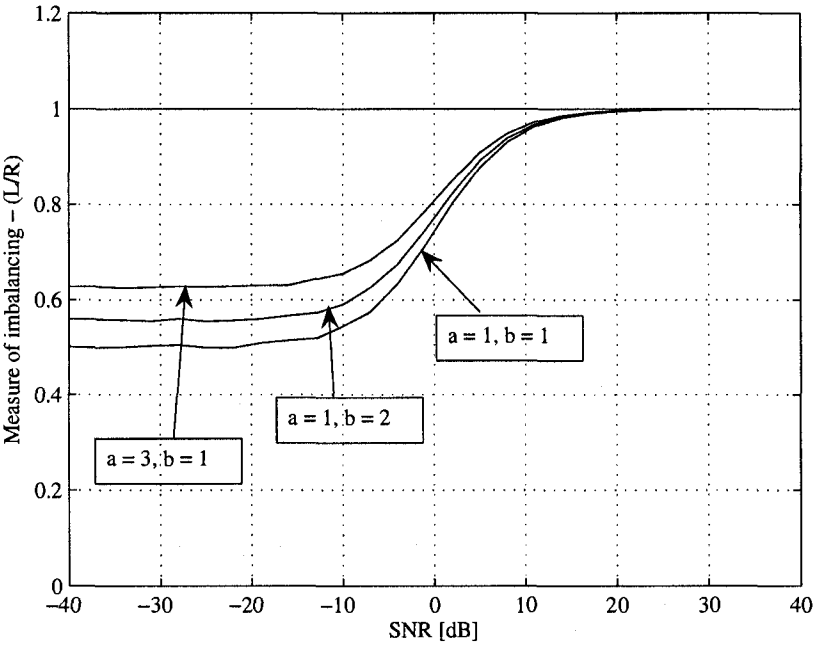

Figure 4.14: Average performance curves for inequality 4.2.4 with (1) $a = b = 1$, (2) $a = 1$ and $b = 2$, (3) $a = 3$, $b = 1$, and $N = 35$.

By examining the performance curves, we can see that they are independent of N. This means that we can estimate the SNR of a sinusoidal signal with a known frequency using the impulse response $h_{g1}[n]$ no matter what the length of the signal is.

4.2.2 Gap of Two

To extend the inequalities further, we consider widening the gap between the non-zero weights to two. Fig. 4.15 shows the impulse response of a system with two circular slots between the two non-zero weights. The process of proof is exactly the same as

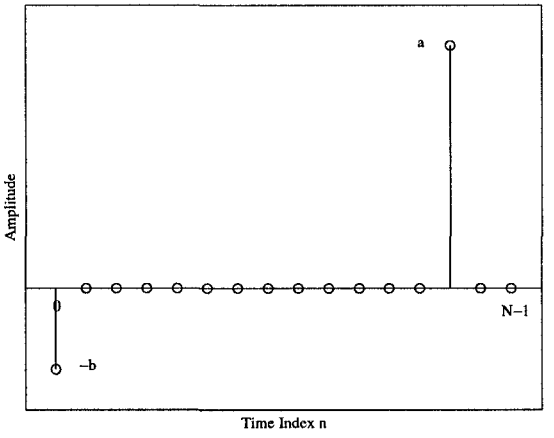

Figure 4.15: $h_{g2}[n]$ - impulse response of the system with two zeros between the two weights.

what was given in Section 4.2.1 for the gap of one. Here we only state the inequalities and avoid repeating the proof steps. The DFT of impulse response $h_{g2}[n]$ is

$$H_{g2}[k] = ae^{j(6\pi/N)k} - b, \quad 0 \leq k \leq N-1, \tag{4.29}$$

and the modulus of $H_{g2}[k]$ is

$$|ae^{j(6\pi/N)k} - b|^2 = a^2 + b^2 - 2ab\cos\frac{6\pi k}{N}, \quad 0 \leq k \leq N-1. \tag{4.30}$$

The extremal values occur when the first derivative is zero, yielding $\sin\frac{6\pi k}{N} = 0$ or $k_i = mN/6$ where $m = 0, \cdots, N-1$ and $i = 1, \cdots, 6$. Therefore, the indices at

which the maximum or minimum occur depend on the residue of N modulo six. Consequently, six cases exist.

1. $N \overset{6}{\equiv} 0$ $(N = 6l)$.

   Fig. 4.16 shows the magnitude of $a^2 + b^2 - 2ab\cos(6\pi k/N)$ for $N = 18$. In this case, the maximum points are $k_1 = N/6$, $k_3 = N/2$, and $k_5 = 5N/6$. The

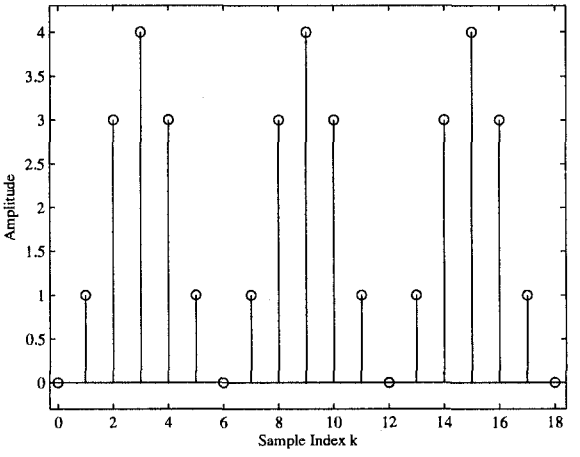

Figure 4.16: $a^2 + b^2 - 2ab\cos(6\pi k/N)$ for $a = b = 1$, and $N = 18$.

inequality is as follows.

Inequality 4.2.5 *For any real signal* $x[n] \in \mathbb{R}^N$, $n = 0 : N-1$, $N = 6l$, *and* $l \in \mathbb{R}$, *the following inequality holds*

$$\sum_{n=0}^{N-1}(ax[n+3] - bx[n])^2 \leq (a+b)^2 \sum_{n=0}^{N-1} x[n]^2,$$

with equality if and only if $x[n] = \hat{x}[n] = A_1(-1)^n + A_2\cos(\pi n/3 + \gamma)$, *where* A_1, A_2 *and* $\gamma \in \mathbb{R}$.

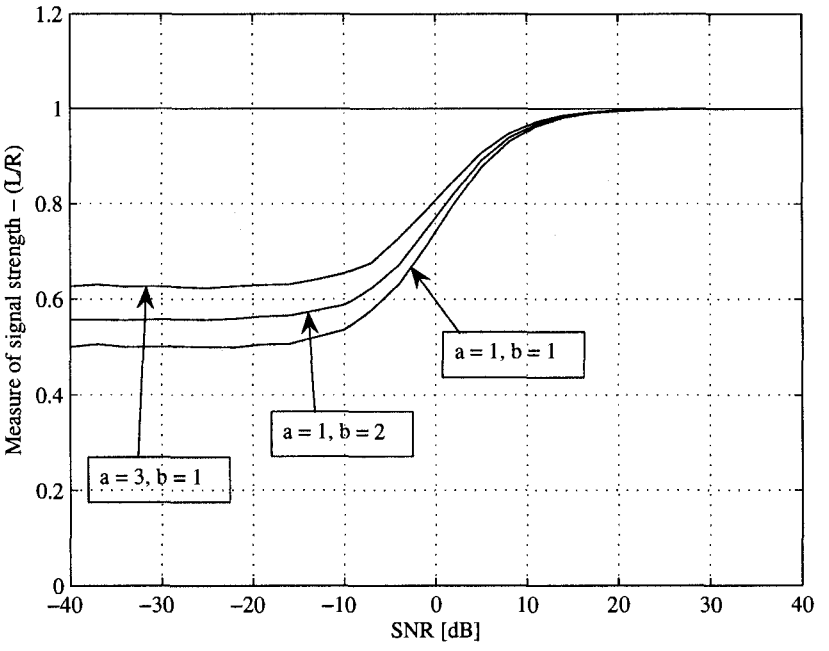

Figure 4.17: Average performance curves for inequality 4.2.5 with (1) $a = b = 1$, (2) $a = 1$ and $b = 2$, (3) $a = 3$, $b = 1$, and $N = 30$.

The performance curves are depicted in Fig. 4.17.

The minimum of $a^2 + b^2 - 2ab\cos(6\pi k/N)$ in this case is zero and the corresponding inequality becomes $\sum_{n=0}^{N}(ax[n+3] - bx[n])^2 \geq 0$, which is trivial.

2. $N \overset{6}{\equiv} 1$ $(N = 6l + 1)$.

The magnitude of $a^2 + b^2 - 2ab\cos(6\pi k/N)$ is depicted in Fig. 4.18. In this case the maximum points are $k_1 = (N-1)/6$ and $k_5 = (5N+1)/6$.

Inequality 4.2.6 *For any real signal* $x[n] \in \mathbb{R}^N$, $n = 0 : N-1$, $N = 6l + 1$,

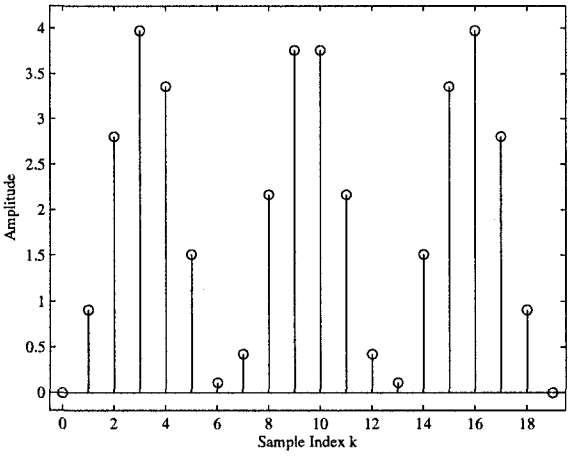

Figure 4.18: $a^2 + b^2 - 2ab\cos(6\pi k/N)$ for $a = b = 1$, and $N = 19$

and $l \in \mathbb{R}$, *the following inequality holds*

$$\sum_{n=0}^{N-1}(ax[n+3] - bx[n])^2 \leq \left(a^2 + b^2 + 2ab\cos(\pi/N)\right)\sum_{n=0}^{N-1} x[n]^2,$$

with equality if and only if $x[n] = \hat{x}[n] = A\cos(\pi n(N-1)/3N + \gamma)$ *where* A, γ $\in \mathbb{R}$.

Three performance curves for inequality 4.2.6 are shown in Fig. 4.19. The minimum of $a^2 + b^2 - 2ab\cos(6\pi k/N)$ in this case is zero and the inequality based on the minimum of $|H_{g2}[k]|$ becomes trivial.

3. $N \overset{6}{\equiv} 2$ $(N = 6l + 2)$.

Fig. 4.20 (a) shows the squared magnitude of $H_{g2}[k]$. In this case, the maximum point is at $k_3 = N/2$.

Inequality 4.2.7 *For any real signal* $x[n] \in \mathbb{R}^N$, $n = 0 : N-1$, $N = 6l + 2$,

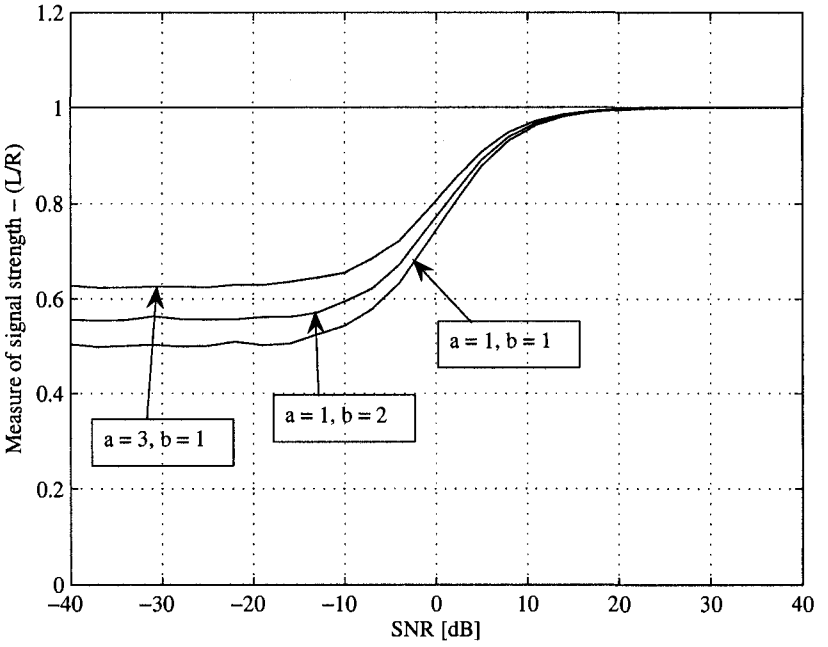

Figure 4.19: Average performance curves for inequality 4.2.6 with (1) $a = b = 1$, (2) $a = 1$ and $b = 2$, (3) $a = 3$, $b = 1$, and $N = 31$.

and $l \in \mathbb{R}$, the following inequality holds

$$\sum_{n=0}^{N-1}(ax[n+3] - bx[n])^2 \leq (a+b)^2 \sum_{n=0}^{N-1} x[n]^2,$$

with equality if and only if $x[n] = \hat{x}[n] = A(-1)^n$, where $A \in \mathbb{R}$.

Fig. 4.21 shows the performance curves for inequality 4.2.7. The minimum of $a^2 + b^2 - 2ab\cos(6\pi k/N)$ is zero and the inequality becomes trivial, if the minimum is taken.

4. $N \overset{6}{\equiv} 3$ $(N = 6l + 3)$.

In this case, we have six maximum points, namely, $k_{1,2} = (N \pm 3)/6$, $k_{3,4} = (3N \pm 3)/6$ and $k_{5,6} = (5N \pm 3)/6$.

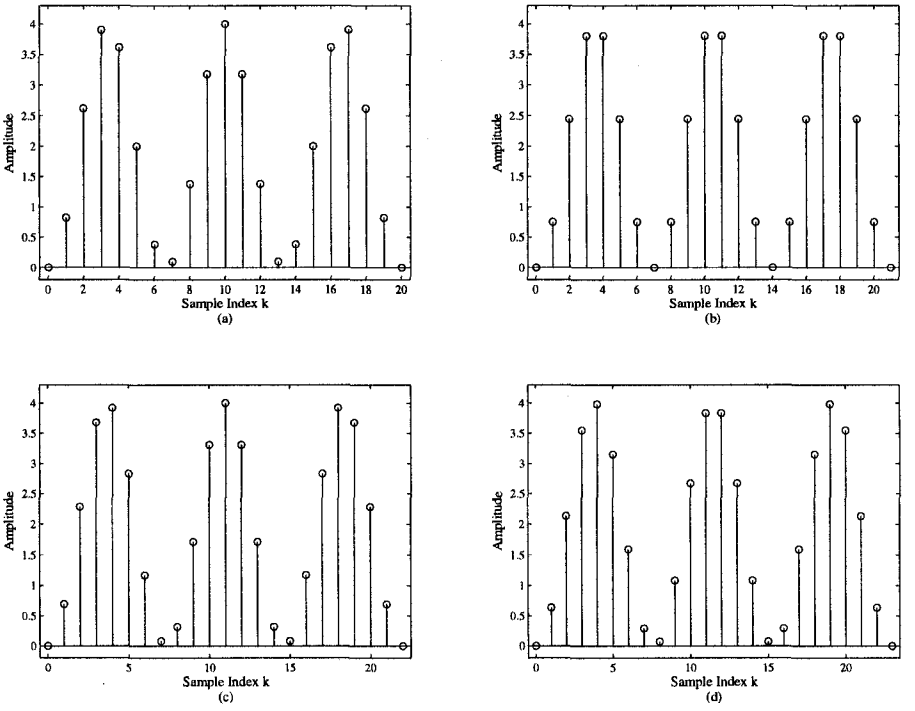

Figure 4.20: (a) $a^2 + b^2 - 2ab\cos(6\pi k/N)$ for $a = b = 1$, $N = 20$, (b) $a^2 + b^2 - 2ab\cos(6\pi k/N)$ for $a = b = 1$, $N = 21$, (c) $a^2 + b^2 - 2ab\cos(6\pi k/N)$ for $a = b = 1$, $N = 22$ and (d) $a^2 + b^2 - 2ab\cos(6\pi k/N)$ for $a = b = 1$, and $N = 23$.

Inequality 4.2.8 *For any real signal* $x[n] \in \mathbb{R}^n$, $n = 0 : N-1$, $N = 6l + 3$, *and* $l \in \mathbb{R}$, *the following inequality holds*

$$\sum_{n=0}^{N-1}(ax[n+3] - bx[n])^2 \leq \left(a^2 + b^2 + 2ab\cos(3\pi/N)\right)\sum_{n=0}^{N-1} x[n]^2,$$

with equality if and only if $x[n] = \hat{x}[n] = A_1\cos(\pi n(N-3)/3N + \gamma_1) + A_2\cos(\pi n(N+3)/3N + \gamma_2) + A_3\cos(\pi n(N+1)/N + \gamma_3)$ *where* A_1, A_2, A_3, γ_1, γ_2 *and* $\gamma_3 \in \mathbb{R}$.

Performance curves are depicted in Fig. 4.22. The minimum is zero and the

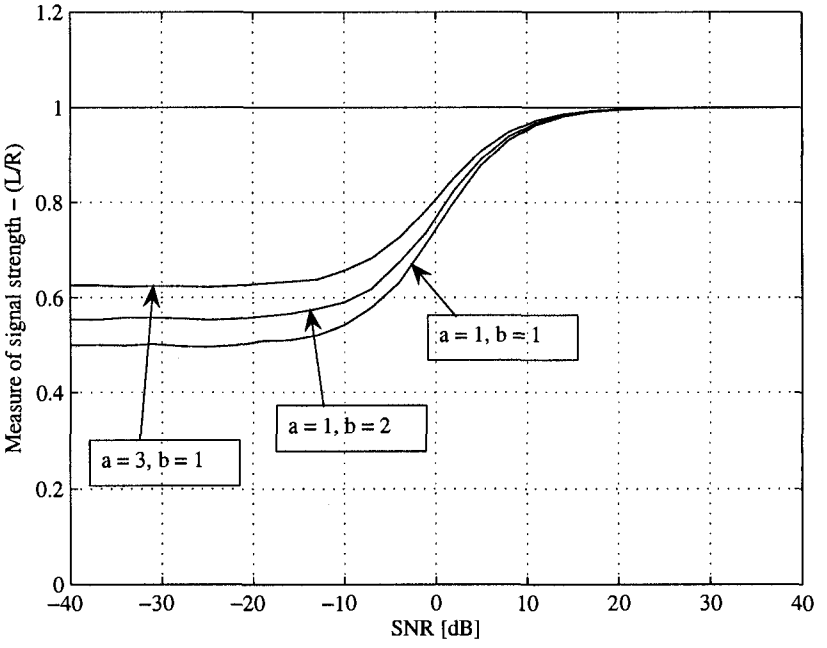

Figure 4.21: Average performance curves for inequality 4.2.7 with (1) $a = b = 1$, (2) $a = 1$ and $b = 2$, (3) $a = 3$, $b = 1$, and $N = 32$.

inequality based on the minimum of $|H_{g2}[k]|$ is trivial.

5. $N \overset{6}{\equiv} 5$ $(N = 6l + 5)$.

In this case, the maximum points are $k_1 = (N + 1)/6$ and $k_5 = (5N - 1)/6$.

Inequality 4.2.9 *For any real signal* $x[n] \in \mathbb{R}^N$, $n = 0 : N - 1$, $N = 6l + 5$, *and* $l \in \mathbb{R}$, *the following inequality holds*

$$\sum_{n=0}^{N-1}(ax[n+3] - bx[n])^2 \leq \left(a^2 + b^2 + 2ab\cos(\pi/N)\right)\sum_{n=0}^{N-1} x[n]^2,$$

with equality if and only if $x[n] = \hat{x}[n] = A\cos(\pi n(N+1)/3N + \gamma)$, *where* A, γ $\in \mathbb{R}$.

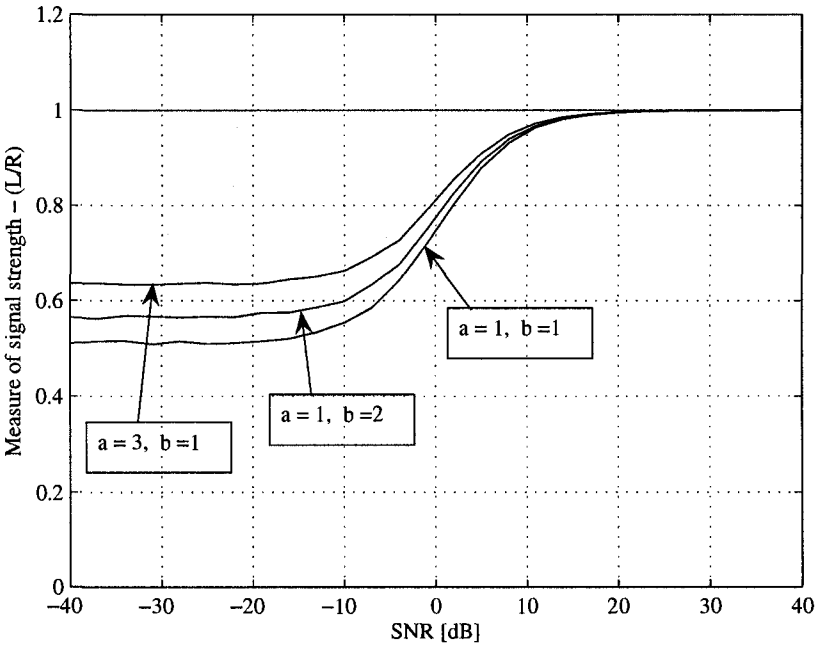

Figure 4.22: Average performance curves for inequality 4.2.8 with (1) $a = b = 1$, (2) $a = 1$ and $b = 2$, (3) $a = 3$, $b = 1$, and $N = 33$.

The performance curves for inequality 4.2.9 are depicted in Fig. 4.23. The minimum of $a^2 + b^2 - 2ab\cos(6\pi k/N)$ in this case is zero and the inequality becomes trivial if the minimum is taken.

Comparison of the performance curves shows that all the curves for the inequalities based on the impulse response with a gap between the two weights are almost the same. Thus, the gap between the weights does not change the performance curve.

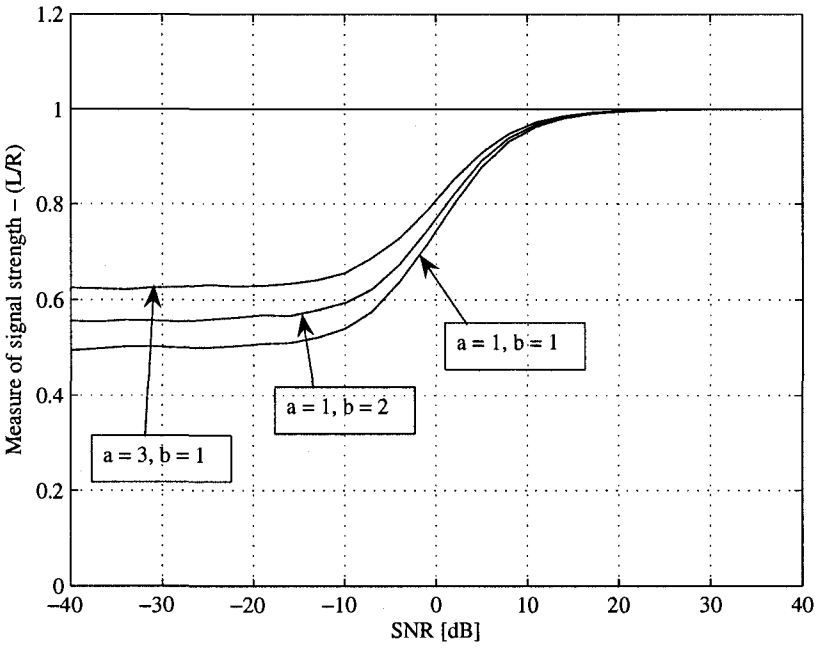

Figure 4.23: Average performance curves for inequality 4.2.9 with (1) $a = b = 1$, (2) $a = 1$ and $b = 2$, (3) $a = 3$, $b = 1$, and $N = 35$.

4.3 Inequalities with Three Non-Zero Weights

In the previous inequalities, we only considered impulse responses with two non-zero weights. As the simulation results show, the performance curves remain unchanged when there is gap between the weights of the impulse response. The problem in finding inequalities for the impulse responses with non-adjacent weights is that the maximum and minimum locations depend on the number of zeros between the weights, which makes working with these inequalities unwieldy. Therefore we are interested in finding inequalities, for impulse responses with three non-zero weights without any gap between them.

Consider the following impulse response

$$h_{3t}[n] = \begin{cases} a, & n = N-2 \\ b, & n = N-1 \\ c, & n = 0 \\ 0, & \text{otherwise.} \end{cases}, \quad 0 \leq n \leq N-1 \tag{4.31}$$

The input-output relationship for this filter is

$$y[n] = ax[n+2] + bx[n+1] + cx[n]. \tag{4.32}$$

Fig. 4.24 shows the impulse response $h_{3t}[n]$. The DFT of $h_{3t}[n]$ is

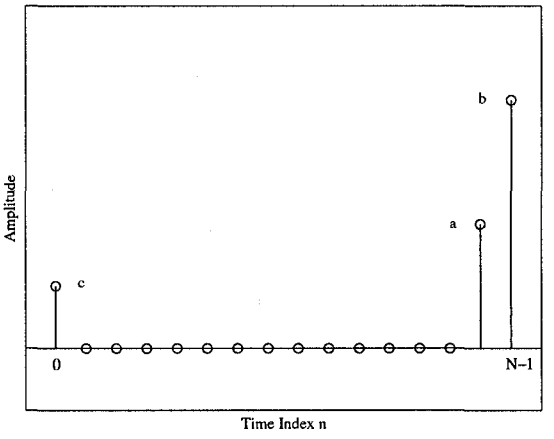

Figure 4.24: Impulse response of the system with input-output relation $y[n] = ax[n+2] + bx[n+1] + cx[n]$.

$$H_{3t}[k] = c + be^{j(2\pi/N)k} + ae^{j(4\pi/N)k}, \tag{4.33}$$

and the modulus of $H_{3t}[k]$ is

$$|H_{3t}[k]|^2 = a^2 + b^2 + c^2 + 2b(a+c)\cos(\frac{2\pi k}{N}) + 2ac\cos(\frac{4\pi k}{N}). \tag{4.34}$$

To find the extremum points, we should solve the following equality

$$\frac{d}{dk}|H_{3t}[k]|^2 = -(4b(a+c)\pi/N)\sin(2\pi k/N) - (8ac\pi/N)\sin(4\pi k/N) = 0. \quad (4.35)$$

It is obvious that the solution of (4.35) depends on the values of a, b, and c. $|H_{3t}[k]|^2$ can have only a maximum and a minimum, a maximum and two minimums, or a minimum and two maximums. Here we only state the case which leads to only one minimum and one maximum.

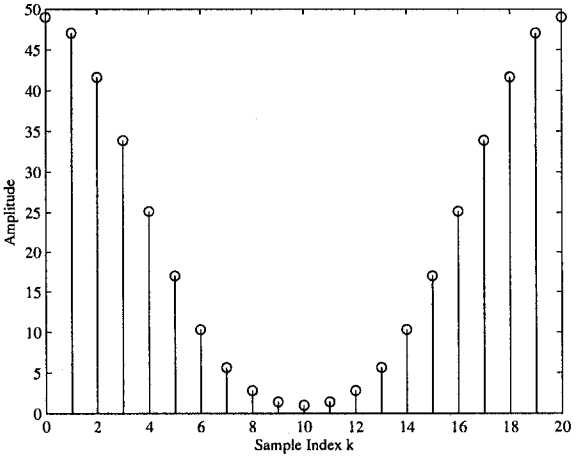

Figure 4.25: $\|H_{3t}[k]\|^2$ with $a = 2$, $b = 4$, $c = 1$, $N = 20$.

Fig. 4.25 shows the moduli of the DFT of the impulse response with one minimum and one maximum. As it can be seen from the graph, the maximum occurs at $k = 0$ and the minimum occurs at $k = N/2$. First, consider the maximum. Since the maximum is located at $k = 0$, we use the embedding as in inequality 3.2.1 where

$$v[i]\Big|_{i=0:2N-1} = (x[0], x[1], \cdots, x[N-1], -x[0], -x[1], \cdots, -x[N-1]). \quad (4.36)$$

The next maximum values occur at $i = 1$ and $i = 2N - 1$ and we have

$$\begin{aligned}&\sum_{i=0}^{2N-1} (av[i+2] + bv[i+1] + cv[i])^2 \\ &\leq \left(a^2 + b^2 + c^2 + 2b(a+c)\cos(\frac{2\pi}{2N}) + 2ac\cos(\frac{4\pi}{2N})\right) \sum_{i=0}^{2N-1} v[i]^2.\end{aligned} \tag{4.37}$$

Expansion of the left side of (4.37) results

$$\begin{aligned}\sum_{i=0}^{2N-1} (v[i+1] - v[i])^2 &= 2\sum_{n=0}^{N-3}(ax[n+2] + bx[n+1] + cx[n])^2 \\ &+ 2(ax[0] - bx[N-1] - cx[N-2])^2 + 2(ax[1] + bx[0] - cx[N-1])^2.\end{aligned} \tag{4.38}$$

It is also clear that $\sum_{i=0}^{2N-1} v[i]^2 = 2\sum_{n=0}^{N-1} x[n]^2$. The equalizing signal therefore can be found by embedding $\hat{x}[n] = A\cos(\pi n/N + \gamma)$, $n = 0 : N-1$. Hence we can state the following

Inequality 4.3.1 *For any real signal* $x[n] \in \mathbb{R}^N$, $n = 0 : N-1$, *the following inequality holds*

$$\begin{aligned}&\sum_{n=0}^{N-3}(ax[n+2] + bx[n+1] + cx[n])^2 + (ax[0] - bx[N-1] - cx[N-2])^2 \\ &+ (ax[1] + bx[0] - cx[N-1])^2 \\ &\leq \left(a^2 + b^2 + c^2 + 2b(a+c)\cos(\frac{\pi}{N}) + 2ac\cos(\frac{2\pi}{N})\right) \sum_{n=0}^{N-1} x[n]^2,\end{aligned}$$

where a, b, *and* c *are positive integers. Equality holds if and only if* $x[n] = \hat{x}[n] = A\cos\left(\pi n/N + \gamma\right)$, *where* $\gamma, A \in \mathbb{R}$.

Fig. 4.26 shows the performance curve for inequality 4.3.1. It can be seen that the non-saturated region is wider and covers more ratio values. In addition, the non-saturated region is more linear than that of the previous inequalities. However, changing the

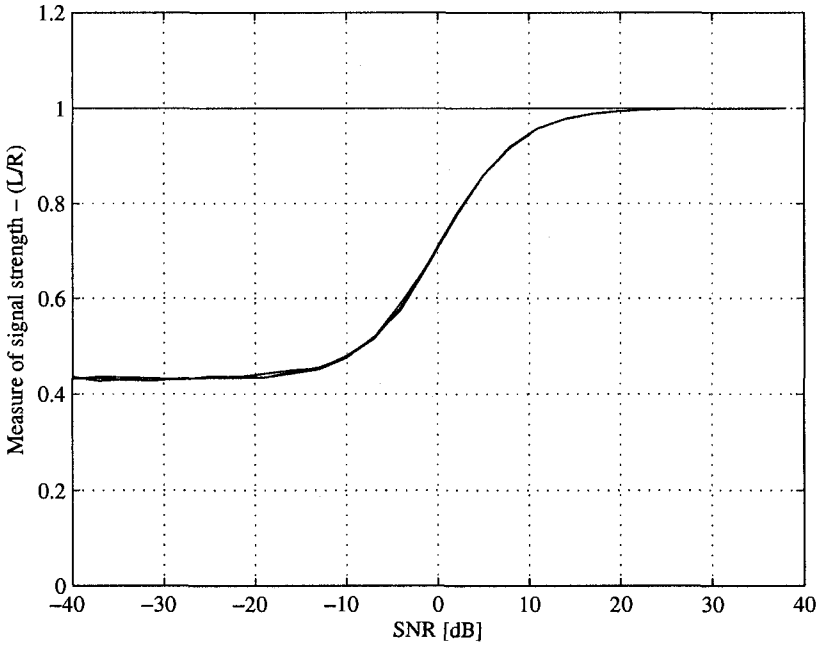

Figure 4.26: Average performance curves for inequality 4.3.1 with (1) $a = 2$, $b = 4$, $c = 1$, (2) $a = 1$, $b = 5$, $c = 3$, (3) $a = 3$, $b = 7$, $c = 2$, with $N = 32$.

weights does not have any effect on the performance curves here. Overall, the performance curves are improved compared to that of the previous inequalities.

Now consider the minimum point. Since the minimum occurs at $k = N/2$, the procedure is exactly the same as inequality 3.2.3, and the following embedding should be performed

$$\begin{aligned} v[i]\Big|_{i=0:2N-1} =& (x[0], x[1], \cdots, x[N-1], \\ & (-1)^{N-1}x[0], (-1)^{N-1}x[1], \cdots, (-1)^{N-1}x[N-1]). \end{aligned} \tag{4.39}$$

Since there is no DFT component of the equalizing signal $\hat{v}[i]$ at $k = 2N/2$, the next

minimum values occur at $i = 2N/2 \pm 1$ and we have

$$\begin{aligned}&\sum_{i=0}^{2N-1}(av[i+2]+bv[i+1]+cv[i])^2\\&\geq\Big(a^2+b^2+c^2-2b(a+c)\cos(\frac{2\pi}{2N})+2ac\cos(\frac{4\pi}{2N})\Big)\sum_{i=0}^{2N-1}v[i]^2.\end{aligned}\tag{4.40}$$

It can be shown that

$$\begin{aligned}\sum_{i=0}^{2N-1}(v[i+1]-v[i])^2 &= 2\sum_{n=0}^{N-3}(ax[n+2]+bx[n+1]+cx[n])^2\\&+2(a(-1)^{N-1}x[0]+bx[N-1]+cx[N-2])^2\\&+2(a(-1)^{N-1}x[1]+b(-1)^{N-1}x[0]+cx[N-1])^2.\end{aligned}\tag{4.41}$$

Consequently, we can state the following result.

Inequality 4.3.2 *For any real signal $x[n] \in \mathbb{R}^N$, $n = 0 : N-1$, the following inequality holds*

$$\begin{aligned}&\sum_{n=0}^{N-3}(ax[n+2]+bx[n+1]+cx[n])^2+(a(-1)^{N-1}x[0]+bx[N-1]+cx[N-2])^2\\&+(a(-1)^{N-1}x[1]+b(-1)^{N-1}x[0]+cx[N-1])^2\\&\geq\Big(a^2+b^2+c^2-2b(a+c)\cos(\frac{\pi}{N})+2ac\cos(\frac{2\pi}{N})\Big)\sum_{n=0}^{N-1}x[n]^2,\end{aligned}$$

where a, b, and c are positive integers. Equality holds if and only if and only if $x[n] = \hat{x}[n] = A(-1)^n\cos\big(\pi n/N+\gamma\big)$, where $\gamma, A \in \mathbb{R}$.

Performance curves for inequality 4.3.2 are depicted in Fig. 4.27. Compared to the previous performance curves, it can be seen that the non-saturated region is wider than that of the previous inequalities.

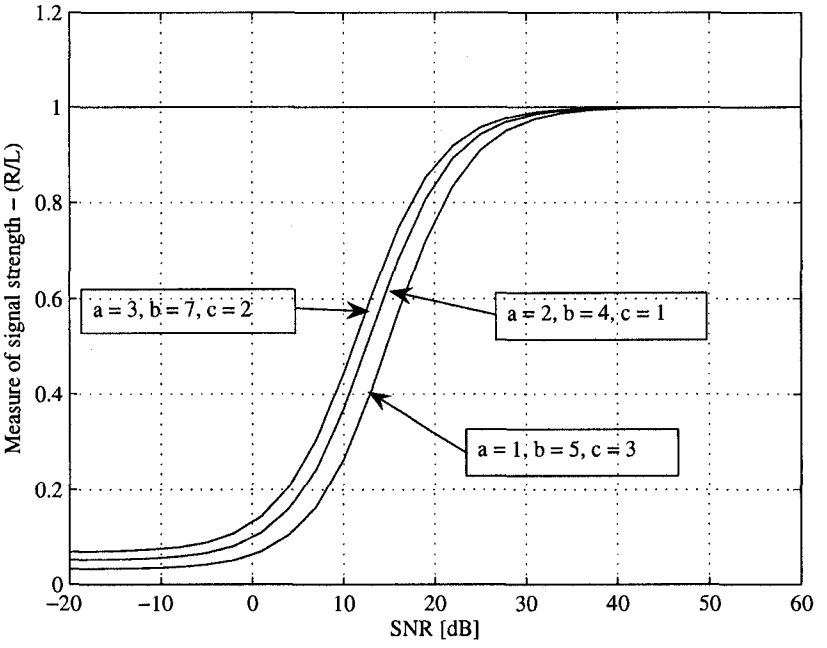

Figure 4.27: Average performance curves for inequality 4.3.2 with (1) $a = 2$, $b = 4$, $c = 1$, (2) $a = 1$, $b = 5$, $c = 3$, (3) $a = 3$, $b = 7$, $c = 2$, with $N = 32$.

4.4 Summary

In this chapter, we generalized the inequalities of Chapter 3. The generalization involved a parametric impulse response. We extended our generalization to the other types of impulse responses with wider gaps between the weights. We also studied the general impulse response with three non-zero weights.

The observations on all the generalized forms of the inequalities leads us to the following important conclusions.

- To obtain a performance curve with a high dynamic range, the best choice is to use inequalities based on the minimum values of the frequency response of the

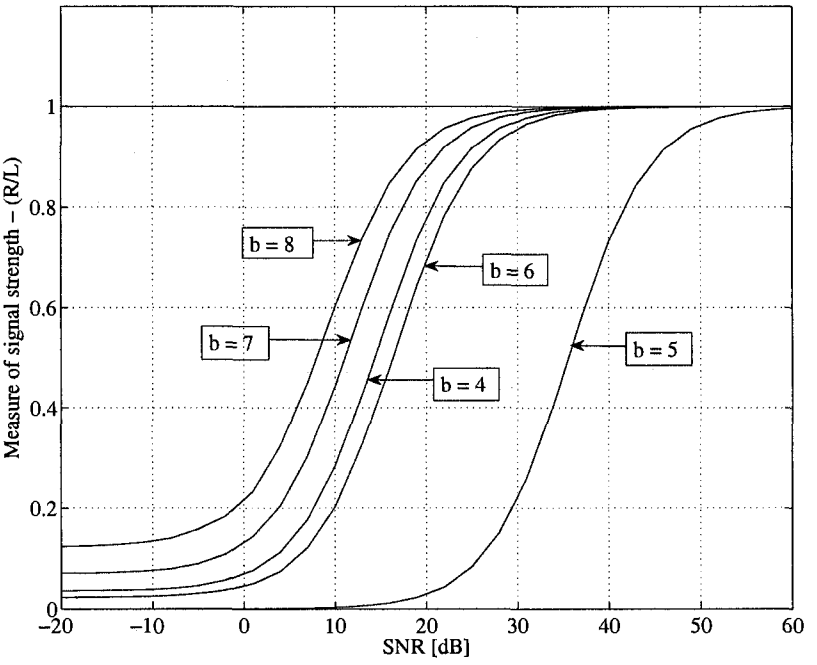

Figure 4.28: Average performance curves for inequality 4.3.2 with $N = 32$, $a = 3$, $c = 2$, and $b = 4, 5, \cdots, 8$.

filter. This will results in a lower ratio at very low SNRs.

- Generalized form of the inequalities allows us to examine the effects of changing the weights of the impulse response on the performance curves. The use of an impulse response with a gap of one and two between the weights does not affect the performance curves significantly. However, different inequalities were derived in these cases that can be used for the SNR estimation of the sinusoids with multiple frequencies.

- The use of impulse response with three weights results in performance curves with a wider non-saturated region that is also more linear than the performance

curves with two weights. Changing the values of the weights of the impulse response in inequalities with three weights may give different performance curves without a significant difference between them.

Comparing the simulation results, it is obvious that to alter the frequency we need a new inequality, which is very hard to find in case of higher frequencies. For instance, the inequalities for gap one involve frequencies $\frac{\pi}{N}$, while by increasing the gap by one, we are able to deal with $\frac{\pi}{2N}$, and by a gap of two we are able to estimate the SNR for $\frac{\pi(N\pm1)}{6N}$. But, for a flexible method, it is necessary to be able to estimate frequencies of the form $\frac{M}{N}\pi$ where $M < N$. In the next chapter, a new method to estimate such higher frequencies is presented and analyzed.

Chapter 5

A Method for Estimating SNR of Sinusoids of Frequency $\frac{M}{N}\pi$ and Its Analysis

In the previous chapter, we saw that in order to make our method more flexible and applicable, we have to find other inequalities which allow us to estimate higher frequencies. However, finding an inequality for estimating a rational multiple of π by changing the gap or weights is a difficult and tedious task. Besides, from the implementation point of view, this is a major restriction because for each frequency a new equality has to be used which makes the method very complicated and inefficient. Our goal is to find a general method that is capable of estimating the SNR of a sinusoid with the frequency $\frac{M}{N}\pi$. The problem we are concerned with is as follows.

Problem. Given a finite-length signal, containing a sinusoid of frequency $\frac{p\pi}{N}$ and arbitrary phase, which has been corrupted with additive white noise, estimate the SNR.

In this chapter, we first describe the basic idea, and then use it to propose a flexible method for SNR estimation based on the inequalities given in the previous chapters.

Consider the following sequence of integers

$$u = \big(0, 1, 2, \cdots, N-2, N-1\big), \tag{5.1}$$

where $N \in \mathbb{N}$. Let $p \in \mathbb{N}$ and $p < N$. Now multiply sequence u by p to create the sequence

$$v = \big(0, p, 2p, \cdots, (N-2)p, (N-1)p\big). \tag{5.2}$$

If p and N are coprime[1], i.e., $\big(p, N\big) = 1$, then the reduction modulo N of sequence v,

$$\big(\ 0,\ ((p))_N\ ,\ ((2p))_N\ , \cdots,\ (((N-2)p))_N\ ,\ (((N-1)p))_N\ \big) \tag{5.3}$$

is a permutation of sequence u [19].

[1]Integers x and y are coprime or relatively prime if their greatest common divisor is 1 or, equivalently, $\gcd\big(x, y\big) = 1$.

5.1 Signal Reordering and Modulation for Frequency Downconversion

Let

$$x[n] = A\cos(M\pi n/N + \gamma) + e[n] \tag{5.4}$$

be the observed signal. We want to estimate the SNR with respect to $A\cos(M\pi n/N + \gamma)$ using the same inequalities that are used for the estimation of the SNR of $A\cos(\pi n/N + \gamma)$. The idea is to convert $x[n]$ to the form

$$x'[n] = A\cos(\pi n/N + \gamma') + e'[n], \tag{5.5}$$

using the permutation property explained in the previous section and a simple modulation involving a change-of-sign operation. Accordingly, we are interested in finding an integer p and an integer-valued function $f[n]$ so that the signal

$$x'[n] = (-1)^{f[n]}x[((pn))_N], \tag{5.6}$$

contains a sinusoid of frequency π/N. Obviously, p and N must be coprime so that a perfect permutation is obtained and the samples are all presented. Since M and N can always be reduced to the simplest form so that they are coprime, the application of Euclid's algorithm results in two integers p and q so that

$$Mp + Nq = 1. \tag{5.7}$$

This way, the integer p used in the permutation of the signal $x[n]$ can be determined. The requirement for a perfect downconversion can be written as the identity

$$(-1)^{f[n]}A\cos(\frac{M((pn))_N\pi}{N} + \gamma) = A\cos(\frac{\pi n}{N} + \gamma'). \tag{5.8}$$

Note that we can write pn as

$$pn = GN + ((pn))_N, \tag{5.9}$$

where G is an integer. Therefore

$$(-1)^{f[n]} A\cos(\frac{M((pn))_N \pi}{N} + \gamma) = (-1)^{f[n]}(-1)^{MG} A\cos(Mp\frac{\pi n}{N} + \gamma). \tag{5.10}$$

Substituting the value of p from (5.7), we have

$$\begin{aligned}(-1)^{f[n]}(-1)^{MG} A\cos(Mp\frac{\pi n}{N} + \gamma) =& (-1)^{f[n]}(-1)^{MG} A\cos((\frac{1}{N} - q)\pi n + \gamma) \\ =& (-1)^{f[n]}(-1)^{MG+nq} A\cos(\frac{\pi n}{N} + \gamma).\end{aligned} \tag{5.11}$$

Consequently

$$f[n] = -(MG + nq) = -\big(qn + \frac{M(pn - ((pn))_N)}{N}\big). \tag{5.12}$$

In order to use the SNR estimation method of the previous chapter for estimating the SNR of $A\cos(M\pi n/N + \gamma)$, first we obtain $x'[n]$ from $x[n]$ by (5.6). Then, we use the same method for estimating the SNR of a sinusoidal signal given in Fig. 3.1. The only information that we need is the value of p and the value of q which are calculated using Euclid's algorithm. Fig. 5.1 shows the SNR estimation method for the solution of the problem stated in the beginning of this chapter in the form of a block diagram.

For instance, consider inequality 4.1.1. Fig. 5.2 shows the simulation results based on the block diagram of Fig. 5.1. It can be seen that the performance curve for estimating the SNR of $\frac{M}{N}\pi$ is almost the same as the performance curve for estimating the SNR of $\frac{\pi}{N}$, as expected. It is important to stress that, with this method we can

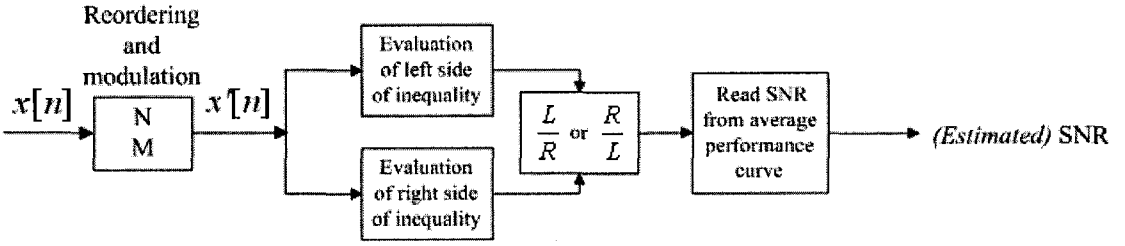

Figure 5.1: Block diagram of the proposed method for estimation of the SNR of a sinusoidal signal with known rational frequency $\frac{M}{N}\pi$.

estimate the SNR of a sinusoid of arbitrary rational frequency $\frac{M}{N}\pi$ using a single inequality depending on N only.

5.2 Optimum Impulse Response Coefficients of The Weighted Forward Difference System

As we saw in Chapter 4, the inequalities can be generalized with two weights a and b. These coefficients determine the shape of the DFT of the impulse response. In addition, by changing the values of a and b certain features of the performance curve, such as the ratio at low SNRs, and the width of the non-saturated region, change as well. Therefore, the effect of variation of these weights on the performance curves of inequalities is of interest.

The maximum or minimum of the moduli of the DFT coefficients of the impulse response determine the equalizing signal for each inequality. Frequencies at which the extrema occur are the frequencies of the equalizing signal. The DFT of the impulse response of the forward difference system can be viewed as a high-pass filter. The

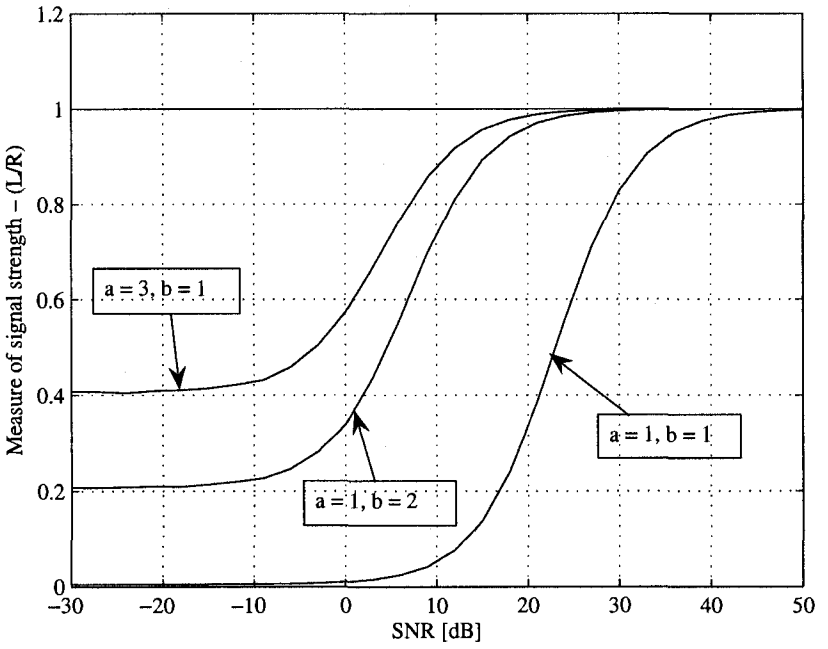

Figure 5.2: Average performance curve for inequality 4.1.1 with (1) $a = b = 1$ (2) $a = 1$ and $b = 2$ (3) $a = 3$ and $b = 1$, with $N = 32$, $M = 5$.

value of the maximum shows how much the filter amplifies signal frequencies around the frequency at which the maximum happens. On the other hand, the value of the minimum mainly determines the attenuation of the noise at its adjacent frequencies. Therefore, the difference between the maximum and minimum values can be viewed as a measure of signal boosting. Moreover, as the minimum tends to zero, the noise power becomes weaker on the left side. Consequently, it is desirable to use the inequalities with the maximum located at the frequency of the equalizing signal and a narrower transition region between the maximum and minimum.

Fig. 5.3 shows the moduli of the DFT of the impulse response $h_{wf}[n]$ of Section 4.1 for several values of a and b. It can be verified that changing a and b has no effect

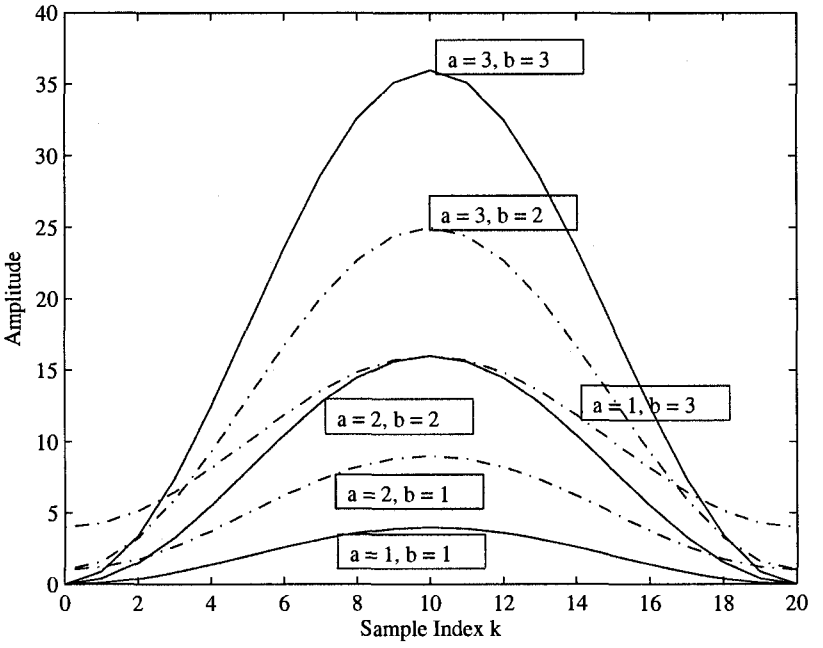

Figure 5.3: $|H_{wf}[k]|^2 = a^2 + b^2 - 2ab\cos(2\pi k/N)$, for $N = 20$ at different values of weights a and b. The dotted curves show the graphs in which $a \neq b$.

on the frequencies where the extrema happen. It is also obvious that the least ratio at low SNRs is attained when $a = b$ because the minimum is zero in that case. Also as the absolute value of a (or b) increases, the difference between the maximum and minimum also increases which result in more signal amplification. However, since $a = b$ the ratio remains constant by increasing the value of a (or b) because the factor

$$a^2 + b^2 - 2ab\cos(2\pi k/N)\Big|_{a=b} = 2a^2(1 - \cos(2\pi k/N)), \tag{5.13}$$

appears in both the numerator and denominator in calculation of the ratio by dividing the two sides of the inequalities.

To study the effect of changing weights on the dynamic range of the ratio in

performance curves, we carried out simulations based on inequality 4.1.1. In our simulations only the ratio b/a is changed. The ratio (R/L) is calculated in each simulation for five different SNR values. The result is shown in Fig. 5.4.

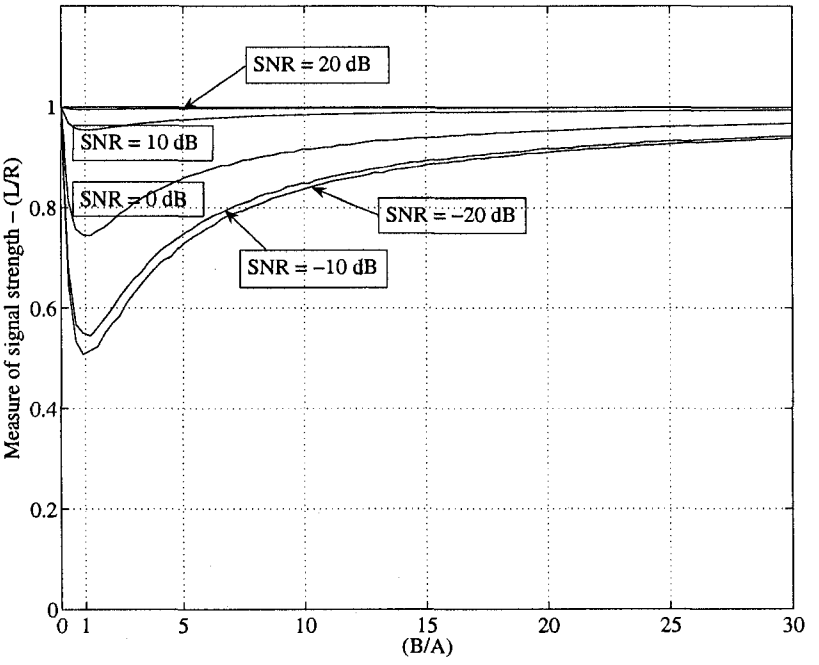

Figure 5.4: Ratio of the two sides of inequality 4.1.1 vs. $\frac{b}{a}$ at different SNR values.

It can be seen from the figure that the ratios at different SNR values are very close when b/a is increased. This is not desirable because at low SNR values we would get almost the same ratio as what we get at high SNRs. On the other hand, the dynamic range of the ratio at different SNR values is higher when $b/a = 1$. This verifies the fact that the optimum coefficients for obtaining the highest dynamic range of the ratio in weighted forward difference system are attained when $b/a = 1$ or $b = a$. However, note that the shape of the performance curve changes with b/a and one might make

other choices to achieve other design considerations.

5.3 Comparison with A Classical DFT-Based Approach

The purpose of this section is to motivate the reader by providing the details of the classical DFT-based approach to the estimation of the SNR of a sinusoid buried in white noise according to the model

$$x[n] = Acos(\frac{n\pi}{N} + \gamma) + e[n]. \tag{5.14}$$

The assumption is that there are only N samples available for $n = 0, 1, \ldots, N-1$. Obviously, even if $e[n] = 0$, the DFT coefficients $X[k]$ are not δ-type functions and spread over the entire range of index k. This makes it difficult to distinguish noise from signal and estimate the SNR. To rectify the situation, we should embed $x[n]$ in the time-domain signal $v[n]$ as

$$v[n]\Big|_{n=0,\cdots,N-1} = (x[0], x[1], \ldots, x[N-1], -x[0], -x[1], \ldots, -x[N-1]). \tag{5.15}$$

Denoting the DFT coefficients of the $2N-1$-point signal $v[n]$ by $V[k]$, we can easily observe that $V[1]$ and $V[2N-1]$ are the only two coefficients that contain the signal information. Based on this observation, we can use the ratio

$$\frac{|V[1]|^2 + |V[2N-1]|^2}{\sum_{k=0}^{2N-1} |V[k]|^2} \tag{5.16}$$

as a measure of signal strength that clearly reflects the SNR value of the observed sinusoid. We can now use numerical simulations to plot a curve that provides SNR

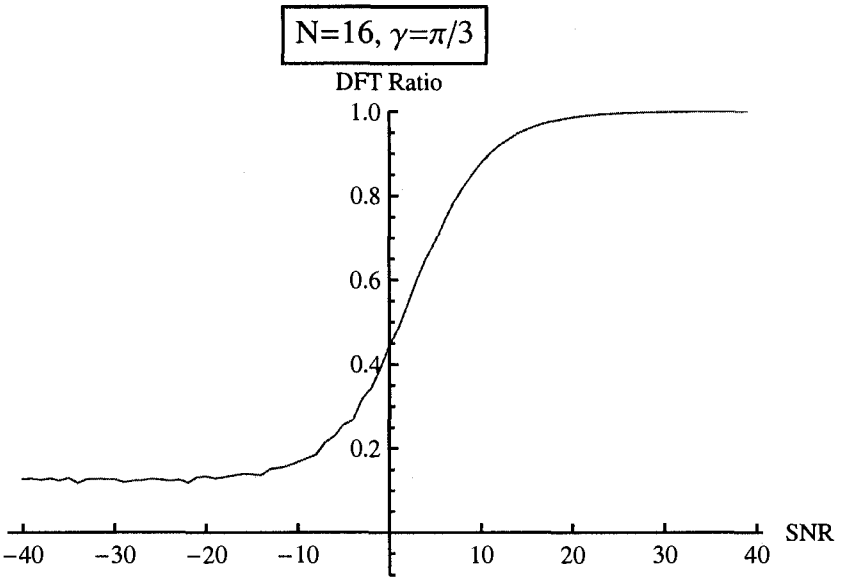

Figure 5.5: Average performance curve for inequality 4.1.1 using a classical DFT-based method for $N = 16$, with $a = b = 1$.

estimates at a given value of the ratio. An example of such performance curves is provided in Fig. 5.5.

5.4 Computational Complexity

In the previous section, we explained how the proposed method of estimation works, and what the trade-offs that we face are when it comes to choosing the right inequality. From an implementational point of view, the computational complexity is of great importance since it determines whether our algorithm is easy to implement, and also how long it takes for the algorithm to execute.

The computational complexity is evaluated based on the amount of resources needed for the execution of an algorithm, such as time, memory, etc. There are

different ways to measure the complexity of an algorithm. However, the final evaluation depends on the technology and the application in which the algorithm is used. Here, we use the number of mathematical operations as a measure of computational complexity of the method. Consider the block diagram of Fig. 5.1. In our proposed two-term inequality, the evaluation of the left side requires $3N$ real multiplications. Further, $N+1$ multiplications are required for the evaluation of the right side of it. Thus the total number of real multiplications becomes $4N+1$. On the other hand, the number of real additions required for the evaluation of the left side and the right side are $2N-1$ and $N-1$, respectively, yielding a total of $3N-2$ additions.

We are interested in comparing the computational complexity of our method to that of the periodogram, since all the other methods of spectrum estimation are usually compared with it. The periodogram method and many other spectrum estimation methods are based on the DFT of the observed data. Therefore, the computational complexity of the periodogram method is determined by that of the DFT. The direct computation of the DFT of a signal $x[n]$ requires $4N^2$ real multiplications and $N(4N-2)$ real additions [11]. Evaluation of a sinusoidal signal's SNR using our method with a filter having three weights requires $5N$ real additions and $4N-2$ real multiplications. Comparing the computational complexity of our method to that of the periodogram shows that our method has a high efficiency in estimating the strength of sinusoidal signals. Other efficient methods exist for computing the DFT of a signal such as Goetzel's algorithm, for which the computation is proportional to N^2, or FFT algorithms requires computation proportional to $N \log N$. However, our method still has a lower computational complexity, since its complexity is propor-

tional to N.

5.5 Analysis of the Error Due to Finite Duration of Observed Signal

In real-world applications, the entire signal is not available in many cases, and a windowed signal is usually observed. The effect of this incomplete observation should be analyzed for any process that uses windowed signal. The effect of windowing is an error generated at the output of the process. In this case, we want to estimate the SNR of a sinusoidal signal with the rational frequency of $M_0\pi/N_0$, modeled as $x[n] = A\cos(M_0\pi n/N_0 + \gamma) + e[n]$, and let N be the length of the observed data. The problem is if we can estimate the SNR when we have only $N < N_0$ samples available. We may be able to estimate the SNR if there is an integer M so that the difference $\left|\frac{M_0}{N_0} - \frac{M}{N}\right|$ is less than ϵ. The smaller the ϵ, the closer the frequencies $M\pi/N$ and $M_0\pi/N_0$ and, consequently, the more accurate and consistent the SNR estimate.

For instance, let the frequency of our signal be $M_0/N_0 = 452/2547$. Table 5.1 shows the fractions M/N that can be used for the estimation of the SNR of the sinusoidal signal $5\cos(452\pi n/2547 + \gamma)$, with the corresponding ϵ. We studied the

$\frac{M}{N}$	$\frac{1}{6}$	$\frac{3}{17}$	$\frac{11}{62}$	$\frac{63}{355}$	$\frac{452}{2547}$
ϵ	10^{-1}	10^{-3}	10^{-4}	10^{-5}	10^{-6}

Table 5.1: Values of ϵ associated with each M/N

estimation method by generating the signal $x[n] = A\cos(452\pi\ n/2547 + \gamma) + e[n]$, $n = 0 : N - 1$, and estimating the SNR using the values of M and N given in the table 5.1. The performance curves are depicted in Fig. 5.6.

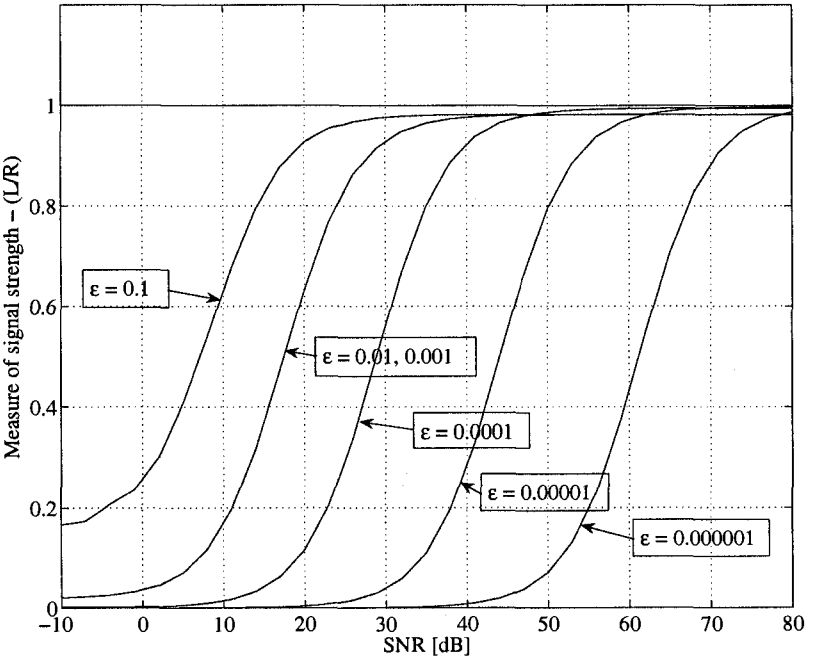

Figure 5.6: Average performance curves for inequality 4.1.1 using different lengths of the observed signal in table 5.1, with $a = b = 1$.

Note that the inequality 4.1.1 is based on the minimum value of the DFT of the filter. According to the performance curves, as N decreases, the curves move to the left. Therefore, when we use fewer samples, the difference between the real SNR and the windowed SNR. This is because of the nature of the inequality which is based on the minimum value of the DFT of the impulse response. It tends to zero as N increases. Hence, the energy of the signal should be very high to balance both sides

of the inequality. Therefore, for inequalities based on the minimum value of the DFT of the filter, windowing results in a significant loss of accuracy in estimating the SNR.

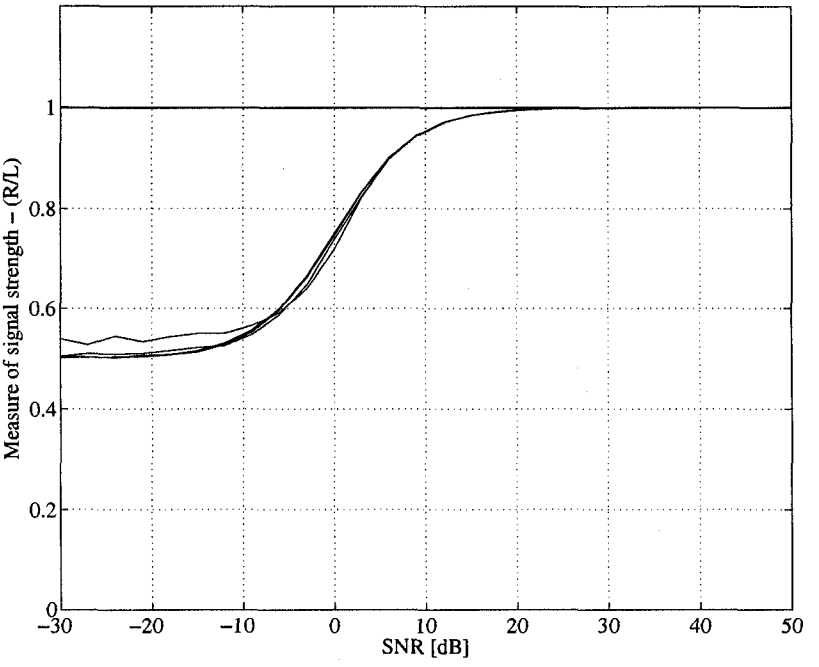

Figure 5.7: Average performance curves for inequality 4.1.3 using different lengths of the observed signal in table 5.1, with $a = b = 1$.

Now consider inequality 4.1.3 which is based on the maximum modulus of the DFT coefficients of the impulse response. Fig. 5.7 shows the performance curves for different values of ϵ. It can be seen that using less samples does not change the performance curve significantly. The curves remain unchanged and the ratio at low SNRs slightly changes. Consequently, we can estimate the SNR with less samples, while reducing the computational complexity, which is proportional to the signal length. However, we should note that in these types of inequalities the estimation

can not be carried accurately at low SNRs. This should be considered when using these types of inequalities with less number of samples.

Chapter 6

Conclusion and Future Work

6.1 Conclusion

The primary contribution of this thesis is the modification and generalization of discrete-time Wirtinger inequalities to allow their application in the SNR estimation of sinusoids. From a mathematical stand point, the results are new and significant. The generalization of discrete Wirtinger-type inequalities is also important in the theory of signal processing. The secondary contribution of our work is the development of a method for estimation of the SNR of a sinusoidal signal with a known frequency of the form $\frac{M}{N}\pi$, buried in additive white noise.

Current methods of spectral estimation have been reviewed briefly. The history of development of Wirtinger type inequalities along with the approaches used for the proof of these inequalities have been mentioned. The inequalities given in Lunter's paper [18] have been presented and proved using a DFT-based approach, and an unnoticed remark on Lunter's results has been elucidated. We studied estimation of the

SNR of a sinusoidal signal of a known frequency, corrupted with additive white noise, and proposed an inequality-based solution method of SNR estimation of sinusoids of frequency $\frac{\pi}{N}$. The drawbacks and limitations of using the existing inequalities in the proposed method have been discussed and the solutions to eliminate the constraints have been developed. The modifications pertaining to the suggested solutions have been carried out and new inequalities have been derived. The estimation method has been studied on the basis of the improved inequalities and the simulation results have been given in the form of performance curves. In order to have a measure of comparison among the performance curves, saturated and non-saturated regions have been defined and compared for the modified inequalities.

In order to study the variations in the performance curves of the modified inequalities and obtain other equalizing signals with different frequencies, generalizations of the modified inequalities have been presented. These include increasing the gaps between the two weights of the filter's impulse response and employing filters with more weights to obtain performance curves with a wider non-saturated region. The effect of changing the weights of the inequality has been also studied. By the use of a permutation property, Euclid's algorithm, and modulation, an arbitrary sinusoid of a known rational frequency $\frac{M}{N}\pi$ has been converted to a sinusoid of frequency $\frac{\pi}{N}$, allowing the proposed method to estimate the SNR of sinusoids of a higher frequencies. Furthermore, the optimum values of the weights for the impulse response having two weights has been obtained. The computational complexity of the proposed method has been evaluated and compared with a DFT-based approach. The effect of windowing on the proposed method has also been discussed. Simulation results showing the

capability of the proposed method in estimating the SNR of an arbitrary sinusoidal signal with rational frequency $\frac{M}{N}\pi$ buried in additive white noise have been provided as various performance curves.

The advantage of the proposed method is that it can be adaptively adjusted to the length of the observed signal, while a DFT-based method should change its weights. However, it should be noted that we are not proposing this method as a replacement to the other powerful estimation methods, but in cases where we desire to evaluate the SNR of an arbitrary sinusoidal signal, this method can be used as a simple and efficient option.

6.2 Future Work

Further development of this work can be carried out in several directions. One of the important aspects is to discover superior digital filters that can be used in the inequalities yielding wider non-saturated regions in the performance curve. The use of more sophisticated digital filters leads to more accurate estimation of the SNR in all ranges.

Another interesting aspect is the use of other classes of inequalities, such as Opial inequalities, to develop an estimation method for other types of signals.

A Possible industrial application of the proposed method can be estimation of the pitch of a received sound. The simplicity and low computational complexity of the method is specially suitable for a hand-held device to be used for training singers and

musicians who need to verify the closeness of sound to a certain tone [1].

[1]We are indebted to professor A. Nishihara and his lab for this suggestion.

References

[1] A. Wiesel, J. Goldberg, and H. Messer-Yaron, "SNR estimation in time-varying fading channels," *Communications, IEEE Transactions on*, vol. 54, no. 5, pp. 841–848, May 2006.

[2] H. Xu and H. Zheng, "The maximum-likelihood SNR estimation algorithm for QAM signals," *Signal Processing, The 8th International Conference on*, vol. 3, pp. –, 16-20 2006.

[3] E. Nemer, R. Goubran, and S. Mahmoud, "SNR estimation of speech signals using subbands and fourth-order statistics," *Signal Processing Letters, IEEE*, vol. 6, no. 7, pp. 171–174, Jul 1999.

[4] P. Stoica, H. Li, and J. Li, "Amplitude estimation of sinusoidal signals: survey, new results, and an application," *Signal Processing, IEEE Transactions on*, vol. 48, no. 2, pp. 338–352, Feb 2000.

[5] M. Chakraborty, H. So, and Z. Jun, "New adaptive algorithm for delay estimation of sinusoidal signals," *Signal Processing Letters, IEEE*, vol. 14, no. 12, pp. 984–987, Dec. 2007.

[6] S. Haykin, *Adaptive Filter Theory.* Upper Saddle River, N.J.: Prentice Hall, 1996.

[7] D. Maskell and G. Woods, "Adaptive subsample delay estimation using a modified quadrature phase detector," *Circuits and Systems II: Express Briefs, IEEE Transactions on*, vol. 52, no. 10, pp. 669–674, Oct. 2005.

[8] S. Bittanti and S. Savaresi, "Safe estimate of sinusoidal signals for control applications," *Decision and Control, 1999. Proceedings of the 38th IEEE Conference on*, vol. 3, pp. 2827–2832 vol.3, 1999.

[9] S. Kay and J. Marple, S.L., "Spectrum analysis: A modern perspective," *Proceedings of the IEEE*, vol. 69, no. 11, pp. 1380–1419, Nov. 1981.

[10] S. J. Orfanidis., *Optimum signal processing : an introduction.* New York: McGraw-Hill, 1988.

[11] A. V. Oppenheim, R. W. Schafer, and J. R. Buck, *Discrete-Time Signal Processing,* 2nd ed. Upper Saddle River, NJ: Prentice Hall, 1998.

[12] R. B. Blackman and J. W. Tukey, *The measurement of power spectra from the point of view of communications engineering.* New York: Dover, 1959.

[13] K. Fan, O. Taussky, and J. Todd, "Discrete analogs of inequalities of Wirtinger," *Monatsh. Math.*, vol. 59, no. 2, pp. 73–90, June 1955.

[14] G. V. Milovanovic and I. Z. Milovanovic, "On discrete inequalities of Wirtinger's type," *J. Math. Anal. Appl.*, vol. 88, no. 2, pp. 378–387, Aug. 1982.

[15] R. P. Agarwal and P. Y. H. Pang, *Opial Inequalities with Applications in Differential and Difference Equations.* Dordrecht, Boston: Kluwer Academic publishers, 1995.

[16] W. Blaschke, *Kreis und Kugel*, Leipzig, 1916, New York, 1949, pp. 13–20.

[17] I. J. Schoenberg, "The finite Fourier series and elementary geometry," *Amer. Math. Monthly*, vol. 57, no. 6, pp. 390–404, June - July 1950.

[18] G. Lunter, "New proofs and a generalization of inequalities of Fan, Taussky, and Todd," *Journal of Mathematical Analysis and Applications*, vol. 185, no. 2, pp. 464–476, July 1994.

[19] R. L. Graham, D. E. Knuth, and O. Patashnik, *Concrete mathematics : a foundation for computer science.* Boston, Mass.: Addison-Wesley, 1994.